

**COAXIAL ADDITIVE MANUFACTURING OF CONTINUOUS CARBON FIBER
COMPOSITES**

by

GİZEM GÖKÇER

Submitted to the Graduate School of Engineering and Natural Sciences
in partial fulfilment of the requirements for the degree of Master of Science

Sabancı University

August 2017

COAXIAL ADDITIVE MANUFACTURING OF CONTINUOUS CARBON
FIBER COMPOSITES

APPROVED BY:

Assoc. Prof. Dr. Bahattin Koç
(Thesis Supervisor)

.....


Assoc. Prof. Dr. Mehmet Yıldız

.....


Prof. Dr. Halit Süleyman Türkmen

.....


DATE OF APPROVAL: 01/08/2017

© Gizem Gökçer, 2017

All Rights Reserved

GİZEM GÖKÇER

IE, M.Sc. Thesis, 2017

Thesis Supervisor: Assoc. Prof. Dr. Bahattin Koç

ACKNOWLEDGEMENTS

I would like to thank many people for the development and completion of this thesis, I learned a lot during this 2-year journey period and I believe all of them will be beneficial for me in the future. I would like to thank Sabancı University, Faculty of Engineering and Natural Sciences (FENS) for supporting me financially through my graduate education.

I would like to express sincere gratitude to my thesis supervisor Bahattin Koç for his help, assistance, encouragements and giving me the opportunity of working on this thesis project. Also, I would like to thank for giving me the chance of being part of the team. I would like to thank all the members of the Koç Group for their nice friendships and supports during my research, especially Cem Dayan and Navid Khani for their help, and Gözde Akdeniz for helping me, transferring knowledge and giving advises. Every time she morally motivated and encouraged me. Also, many thanks to Özlem Karahan for her great help, friendship, and motivation through my research.

I would like to express many acknowledge to the Machine Shop, especially Ertuğrul Sadıkoğlu for his endless support and continuous help. Additionally, special thanks to Sabancı University Integrated Manufacturing Technologies Research and Application Center (SU-IMC), especially Mehmet Olcaz and Çağdaş Akalın for their time, help, transfer of knowledge and supports through my experiments. They encouraged and motivated me a lot through my research, and I had a chance to learned a lot.

Lastly, I would like to thank my family and friends for their endless encouragements, confidence, supports, and motivations. Their supports have always encouraged me for going further.

ABSTRACT

Additive Manufacturing (AM) or 3D Printing, is an emerging technique which produces complex and detailed parts layer by layer. Fused deposition modelling (FDM) is one of the most commonly used AM technique due to its wide usage areas and its low cost. However, FDM applications are generally restricted to prototyping because the process is limited with certain thermoplastic polymers. The thermoplastics used in this process could be inadequate due to their weak mechanical properties. Parallel with the recent developments, there is an emerging need for mechanically stronger and durable parts to broaden the application areas of AM as a functional end-parts. To increase the mechanical performance and usability of the printed parts, composite printing can be used. With the inclusion of the continuous carbon fiber reinforcement to the thermoplastic polymers in a composite form, 3D printed parts could meet the needs by providing increase in the mechanical performance.

This thesis aims to present FDM based coaxial additive manufacturing of continuous carbon fiber reinforced thermoplastic (PLA) composites for improving the mechanical properties of the 3D printed parts compared to pure thermoplastic materials. The effect of embedding continuous carbon fiber as a reinforcement and PLA, in the form of a pellet, as a thermoplastic matrix material is examined experimentally. A special coaxial nozzle, which supplies the continuous carbon fiber and PLA pellets separately, is developed for printing continuous carbon fiber reinforced thermoplastic composites. After the 3D printing process, the tensile and flexural (3-point bending) mechanical tests are conducted. Also, to improve the bonding of the continuous carbon fiber with the thermoplastic polymer, oxygen plasma, which is one of the surface treatment technique, is implemented as pre-processing operation. In addition, as a post-processing technique, a microwave post-processing is used to enhance the bonding of the printed samples and improve the mechanical properties. Scanning electron microscope (SEM) and optic microscope are used for the visual characterization of the printed composite samples.

The results from the mechanical tests showed that continuous carbon fiber reinforced PLA composite resulted in higher tensile and flexure test values than pure PLA. However, adhesion problems were observed, which is one of the main problems with carbon fiber usage in 3D printing, and this limits the much more improved mechanical properties.

ÖZET

Eklemeli Üretim, günden güne gelişen, kompleks şekilleri tabaka tabaka, doğrudan bilgisayar destekli modellerden 3 Boyutlu (3B) yazıcılar ile basılmasını sağlayan bir teknolojidir. Eriyik yığıma modelleme (FDM) tekniği, Eklemeli Üretim metodları içerisinde en çok kullanılan tekniklerden biridir. Fakat, termoplastik malzeme kullanılması ve mekanik özellikler olarak çok güçlü olmayışları nedeniyle, bu yöntemin kullanım alanları prototip oluşturulması olarak kısıtlanmıştır. Örneklerin mekanik özelliklerini iyileştirmek için ve kullanım alanlarını prototip oluşturulması amaçlı kullanımı dışında, daha aktif bir şekilde birçok alanda son ürün olarak kullanabilmek adına, 3B kompozit basım yöntemi kullanılabilir. Buna ek olarak, sürekli formda karbon fiber kullanılarak güçlendirilmiş termoplastik malzeme basımı sayesinde, mekanik olarak çok daha güçlü parçalar üretilebilir.

Bu tez çalışması, sürekli formda karbon fiber filament ile güçlendirilmiş Polilaktik Asit (PLA) termoplastik polimer malzemesi ile kompozit basımı gerçekleştirerek, tek malzemeli basımlara göre mekanik olarak çok daha güçlü parçalar üretebilmeyi hedeflemektedir. Çalışmalar sırasında, malzemeleri güçlendirme amaçlı sürekli formda karbon fiber kullanımının, mekanik olarak etkisi incelenmiştir. İlk olarak, sürekli formda karbon fiberin ve PLA' in ayrı ayrı eklenebileceği basım kafası üretilmiştir ve 3 boyutlu basımlar bu geliştirilen basım kafası ile gerçekleştirilmiştir. Basımlar sonrasında çekme ve 3 nokta eğme testleri yapılmıştır. Ek olarak, sürekli formda karbon fiber ve PLA arasındaki bağlılığı ve yapışmayı arttırabilmek için, basım öncesi ön işlem olarak, oksijen plazma yöntemi kullanılmıştır. Ayrıca, basım sonrası işlemi olarak, mikrodalga fırın kullanılarak, basılan numuneler arasındaki bağlanma gücü arttırılmaya çalışılmıştır. Taramalı elektron mikroskopu (SEM) ve optik mikroskop sayesinde basılan numunelerin görsel karakterizasyonu yapılmıştır.

Yürütülen tez çalışması sonrasında elde edilen sonuçlar, sürekli formda karbon fiber ile güçlendirilmiş PLA kompozit basımının, güçlendirilmemiş PLA basımına göre mekanik olarak çok daha iyi sonuçlar verdiğini göstermektedir. Çalışmalar sırasında, karbon fiber ile basımlarda genel olarak karşılaşılan problem olarak, kompozit malzemelerin yapışma ve bağlanma sorunu gözlenmiştir. Bu problem, mekanik olarak çok güçlü bir artış görmemizi engellemiştir.

To my loving family

Table of Contents

ACKNOWLEDGEMENTS	ii
ABSTRACT	iii
ÖZET.....	iv
LIST OF FIGURES	viii
1. INTRODUCTION.....	1
1.1 Additive Manufacturing (AM)	1
1.2 Fused Deposition Modelling (FDM)	4
1.3 Materials used in FDM	7
1.4 Reinforced materials in FDM	11
1.4.1 Continuous carbon fiber reinforced material in FDM	13
1.4.2 Problems on continuous carbon fiber	19
1.5 Coaxial Printing.....	20
1.6 Objectives for this project.....	21
2. EXPERIMENTAL DESIGN & METHODOLOGY.....	22
2.1 Overview of the Methodology.....	22
2.2 Design and development of the coaxial nozzle	23
2.2.1 Design for the carbon fiber reinforced thermoplastic printing	23
2.2.2 Design modification for pure PLA printing.....	25
2.3 Equipment used and materials	26
2.3.1 Electrical and mechanical equipment	26
2.3.2 Materials	28
2.4 Experimental Setup & 3D printing.....	30
2.4.1 Experimental Setup and procedure	30
2.4.2 3D Printing preparation and process.....	33
2.5 Oxygen plasma as pre-processing technique for carbon fiber.....	38
2.6 Mechanical Tests Methods	40
2.6.1 Tensile Test.....	40

2.6.2 Flexural Test	42
2.7 Tensile following microwave oven application as post-processing	43
3. RESULTS & DISCUSSIONS	44
3.1 Printed parts qualitative characterisation.....	44
3.1.1 Scanning electron microscopy (SEM) imaging of printed parts.....	46
3.1.2 Scanning electron microscopy (SEM) imaging of oxygen plasma technique	49
3.2 Mechanical Tests	50
3.2.1 Tensile test	50
3.2.2 Flexural test	53
3.2.3 Tensile following microwave oven application.....	56
3.2.4 Oxygen plasma application.....	59
3.3 Fracture analysis of the tested samples.....	60
4. CONCLUSIONS & FUTURE WORKS	65
References	67

LIST OF FIGURES

Figure 1: Bar-chart graph analysis on companies utilization of AM [33].	2
Figure 2: Graph of the patent numbers of AM, with years [50].	2
Figure 3: AM usage distribution [29].	3
Figure 4: FDM printing process illustration [14].	4
Figure 5: Representation of staircase effect based on layer thickness [44].	9
Figure 6: Cross section views of the 6-layered carbon fiber (left) and 2-layered carbon fiber (right) [36].	14
Figure 7: Feeding mechanism of the materials; PLA (top) and continuous carbon fiber (side) [37].	15
Figure 8: Tensile modulus (left) and tensile strength (right) comparisons of PLA, JFRTP and CFRTP [37].	15
Figure 9: Printed sample with carbon fiber reinforced PLA material [39].	16
Figure 10: Printed carbon fiber and PLA filament with their dimensions [38].	16
Figure 11: Samples without (upper) and addition (lower) of the thermal bonding process [51].	17
Figure 12: Presentation of die swelling [31].	18
Figure 13: The cross-section area of coaxial printing, internal and external material, top view [30].	21
Figure 14: Overview of the conducted methodology.	23
Figure 15: The initial design of the coaxial nozzle with 3 components and cap, fully assembled view.	24
Figure 16: Final design of the nozzle.	25
Figure 17: Manufactured part for printing pure PLA , Figure 18: Design comparisons for pure PLA (left) and continuous carbon fiber (right).	26
Figure 19: Technical data sheet of the Continuous Carbon Fiber 3K A-38, supplied from AKSACA [52].	28
Figure 20: SEM images of continuous carbon fiber. (A) and (B) presents the obtained measurements, (C) and (D) presents single and two carbon fiber views, respectively.	29
Figure 21: Technical data sheet of the PLA 4043D pellets, supplied from NatureWorks LLC. MD: machine direction and TD: transverse direction [58].	30

Figure 22: The developed experimental setup.	32
Figure 23: General view of the procedure conducted.	33
Figure 24: Cross-sectional view of the coaxially extruded materials. (A) and (B) presents coaxially extruded carbon fiber (core) and PLA4043D (shell), with 5X magnification. (C) and (D) presents coaxially extruded carbon fiber (core) and PCL (shell), with 5X magnification.	34
Figure 25: 3D printing process of the continuous carbon fiber and PLA 4043D, starting from the (A) and continues with (B), (C), (D), respectively.	36
Figure 26: 3D printing with continuous carbon fiber and PLA 4043D. (A) closer view of continuous carbon fiber and PLA 4043D materials, (B) overall view of the 3D printing.	36
Figure 27: 3D printing of pure PLA 4043D. Starting from (A) and continues with (B), (C) and (D), respectively.	37
Figure 28: Printing path for the Tensile test specimen.	38
Figure 29: Printing path for the Flexural test specimen.	38
Figure 30: Torr International Inc. machine, used for oxygen plasma.	39
Figure 31: ASTM D638 standard dog-bone sample' dimensions [53].	40
Figure 32: Instron tensile testing machine with the testing sample.	41
Figure 33: Prepared samples with 0,5 mm aluminium tab. (A) Continuous carbon fiber reinforced PLA samples, (B) Pure PLA samples.	42
Figure 34: Flexural testing machine, with testing sample.	42
Figure 35: 3D printed continuous carbon fiber reinforced PLA samples.	44
Figure 36: 3D printed pure PLA samples.	45
Figure 37: Printed samples with the problem of adhesion. (A) adhesion problem between the stripes, (B) weak bonding and void problems.	46
Figure 38: SEM cross-sectional view of 2-layered carbon fiber reinforced and pure PLA. (A) carbon fiber reinforced PLA sample, (B) pure PLA sample, (C) carbon fiber reinforced PLA sample.	48
Figure 39: SEM image of the Normal (untreated), 2 minutes treated and 3 minutes treated continuous carbon fiber. (A) untreated fiber in general perspective, (B) untreated carbon fiber, (C) 2 minutes treated carbon fiber, and (D) 3 minutes treated carbon fiber.	49
Figure 40: Tensile strength comparison of pure and continuous carbon fiber reinforced PLA' mean values.	50
Figure 41: Tensile strength comparison with different printing parameters of continuous carbon fiber reinforced PLA samples.	51

Figure 42: Tensile strength comparison with different printing parameters of pure PLA samples.....	52
Figure 43: Tensile strength comparison of pure (left) and continuous carbon fiber reinforced PLA (right), with the parameters of; Nozzle 163°C, syringe 170°C, Pressure of 1.8 bar and Feed rate of 120 mm/min.	52
Figure 44: Load vs. Extension comparison of pure and continuous carbon fiber reinforced PLA, with the parameters of; Nozzle 163°C, syringe 170°C, Pressure of 1.8 bar and Feed rate of 120 mm/min.	53
Figure 45: Flexural stress and strain comparison of pure PLA samples.....	54
Figure 46: Flexural stress and strain comparison of continuous carbon fiber reinforced PLA samples, with various printing parameters.	54
Figure 47: Flexure strength comparison of pure (left) and continuous carbon fiber reinforced PLA (right), with the parameters of; Nozzle temperature of 150°C, syringe temperature of 165°C, P 1.5 bar and F 120 mm/min.....	56
Figure 48: Tensile strength comparison of without microwave (left) and microwave treatment (right) for the parameters of Nozzle temperature of 156°C, syringe temperature of 165°C, P 0.7 bar and, F 120 mm/min.	57
Figure 49: Tensile strength comparison of without microwave (left) and microwave treatment (right) for the parameters of Nozzle temperature of 145°C, syringe temperature of 168°C, P 0.5 bar and, F 120 mm/min.	57
Figure 50: Tensile strength comparison of without microwave (left) and microwave treatment (right) for the parameters of Nozzle temperature of 160°C, syringe temperature of 173°C, P 0.55 bar and, F 120 mm/min.	57
Figure 51: Tensile strength comparison of the untreated and the microwave treated continuous carbon fiber reinforced PLA samples.....	58
Figure 52: Tensile strength comparison of untreated (left), oxygen plasma 3 minutes treated (middle), and oxygen plasma 2 minutes treated (right) cases, for the same printing parameters of; Nozzle temperature of 163°C, syringe temperature of 170°C, P 1.8 bar and, F 120 mm/min.	59
Figure 53: Possible tensile tested samples' failure scenarios and their codes [56].....	61
Figure 54: Tensile tested carbon fiber reinforced PLA samples' fractures. (A) PLA cracks on surface and fibers are damaged, (B) PLA fractures and fiber pull-outs on the sides, and (C) fiber explosion.....	62
Figure 55: Without tabbed trial sample's observed fracture.	63

Figure 56: Flexural tested fractures. (A) pure PLA, and (B) continuous carbon fiber reinforced PLA samples. 63

Figure 57: Tensile tested samples' fracture with the microwave oven usage as a post-processing technique. 64

Figure 58: (A) fiber breakages observed in the tensile test with the magnitude 5X, (B) and (C) fiber breakages observed in the flexural test with magnitude 5X, in different perspectives and (D) fiber pull-out case in flexural test with magnitude 10X. 64

Figure 59: Presentation of spread-out continuous carbon fiber. 66

1. INTRODUCTION

1.1 Additive Manufacturing (AM)

Additive Manufacturing (AM) or 3D Printing, is an emerging manufacturing technique which produces complex and detailed parts in the form of layer by layer, directly from the 3-dimensional Computer-Aided Design (CAD) models. Compared to subtractive manufacturing techniques, which have a working principle of removing materials by conventional methods, additive manufacturing is based on a layer by layer deposition, resulted in a minimum waste of the material and great energy and time-savings [28, 29]. Berman [42] reported that, additive manufacturing can decrease 40% material waste when compared with subtractive manufacturing techniques. Some of the advantages of AM are; able to manufacture complex designs and bring huge customization and rapid modifications to the designs. Because the process is digital using computer models, designs can be easily shared among engineers, companies, and customers to make necessary modifications [42]. Hence, Additive Manufacturing can be called as “new industrial revolution”, which helps to integrate computer-based data and design with manufacturing, can have great benefits on the process. Initially, Additive Manufacturing mainly called as Rapid Prototyping (RP), which has a title directly coming from prototype development. However, with the recent developments, this accelerating layer based manufacturing technique started to be called as Additive Manufacturing, rather than using the term Rapid Prototyping [29].

Although AM has great advantages, currently it has some limitations. Some of the important limitations are as follows: i) restricted AM materials, ii) rough surface finish of the parts, which requires post-processing methods, iii) limited mechanical performance of the additively manufactured parts [42].

Additive Manufacturing has a growing, wide range of potential application areas. Currently, global market mainly focuses on fully meeting customer demands on time, with ensuring the quality and mechanical properties of the parts. Additionally, energy and expenses (material and labour force) saving become more critical [29]. Turner et al. [31] underlined in his study that; according to the 2010 Wohler’s report, the additive manufacturing market reached approximately \$1.4 billion. But, by 2020, this number is estimated to rise greatly and can reached to \$5 billion. Based on the conducted analysis in 2014 [33], which discusses the

utilization of additive manufacturing, the analysis results are presented that the most commonly used application is in prototyping and functional testing as shown in Figure 1. However, it is important to note that, approximately 34% of the companies are not benefited from AM yet.

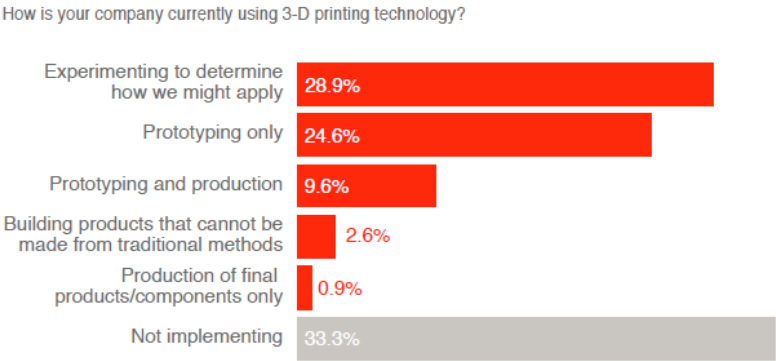


Figure 1: Bar-chart graph analysis on companies utilization of AM [33].

As the graph indicates, one of the highest percent value can be seen in the prototype usage and least percent value in the end-part production. Berman [42] supported this point by giving the example of; with the help of implementing AM as prototype applications, Timberland, which is shoe manufacturer company, can able to manufacture designed models in 90 minutes with the huge amount of money saving. Depending on the improvements and studies on AM, the application of this technology can become widespread and started to take place in different sectors. Hence, developments related to AM and application of relevant patents, are started to accelerate day by day. A graph of the improvement on AM patents with years (1995-2013), is presented in Figure 2. It can be observed that as years passed, the number of patents has also increased.

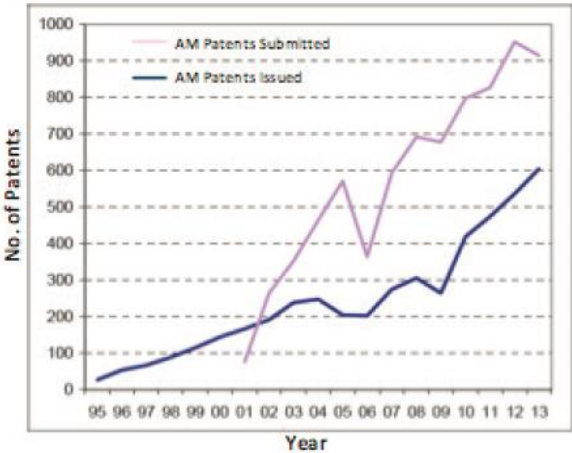


Figure 2: Graph of the patent numbers of AM, with years [50].

Some of the application areas of AM are: biomedical, automotive, aviation, art-design, aerospace, food, clothing and fashion industry. The distribution of the application areas of AM technology can be seen in a pie chart, from Figure 3. As seen from the chart, the highest percentage values are from; consumer products, motor vehicles and medical/dental applications, respectively.

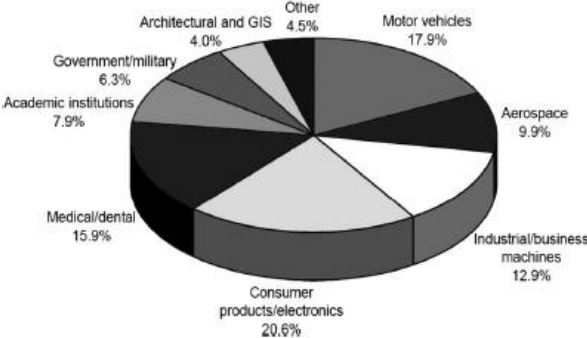


Figure 3: AM usage distribution [29].

Beyer [29] stated in his article that, around 2050’s, plane and rocket components can be additively manufactured, which can result in great advantages in the aerospace area. One of the biggest advantages of AM in aerospace is to produce lighter parts with good mechanical properties [33]. As an example of achieving lighter parts with AM, airplane seat belt design is modified for using conventional and AM methods. The new redesign part for AM resulted in 55% decrease in the weight for one belt compared with the conventional design. Hence, considering a total number of seat belts (around a total of 850 pieces), a weight decrease of around 73 kg can be achieved, which has an immense potential of saving energy, time and money [50]. In the automotive industry, AM is also commonly used for prototyping and customization of parts with the reduction of weight [50].

Another AM application area is in medical and dental sectors. Patient-specific implants can be designed and additively manufactured, which increases the compatibility between the designed implant and patient’s body and enables freedom of motion, minimize possible errors and resulted in best-fit design [33].

Also, with the help of AM, less inventory is required in the warehouses and this directly leads a cost reduction [29], and hence, less stocks are needed which can result in a reduced storage cost [42].

Some of the widely used additive manufacturing techniques are Fused Deposition Modelling (FDM), Stereolithography (SLA), Selective Laser Sintering (SLS) and Selective Laser Melting (SLM) [14]. Additive manufacturing techniques differentiates from the each other depending on what kind of materials used and how these materials are processed [14].

1.2 Fused Deposition Modelling (FDM)

One of the best known additive manufacturing methods is Fused Deposition Modelling (FDM), which was first introduced by Stratasys around 1980s [23, 24].

In FDM technology, thermoplastic filament material forced out by the extruder and material is melted by using a heater. Semi-molten state polymer is deposited layer by layer onto a printing bed. Before the printing process, the deposition locations need to be determined and controlled by moving the nozzle in the direction of the x-y-z plane on the platform. The process controlled by using software which is connected to the platform and the instructions are required to specify the printing coordinates, parameters, and movements. At the end of the completion of each layer, the bed is lowered in the z-direction as defined by the layer thickness, and the layer deposition is continued with the next layer. This procedure continues until the completion of the part. When the material is deposited onto the printing bed, it started to get solidified [5,10,31]. Apart from the printed material, the support material can also be used, depending on the printed parts' geometry to support the process. At the end of the printing process, the support material can be broken or removed [35]. FDM process can be seen as described in Figure 4.

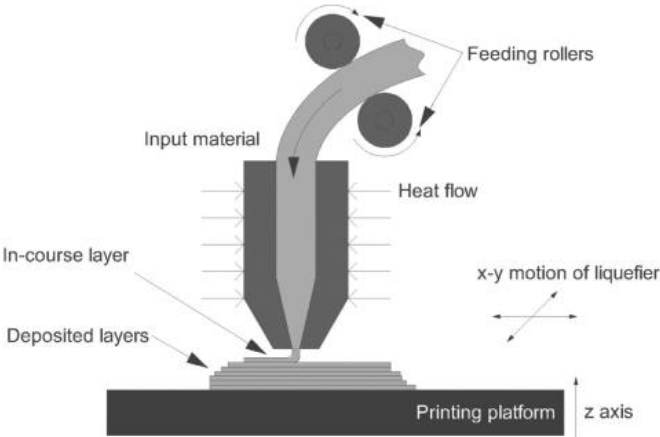


Figure 4: FDM printing process illustration [14].

FDM is generally used for prototype applications because the process is limited with small part sizes. Also, FDM process has long processing time with low deposition rate that can directly restrict the usability of the process. Commonly used FDM materials such as PLA and ABS do not have great mechanical properties, and improvements are needed to have better mechanical abilities that can increase the usability of the process in different application areas [9, 24].

To address against the restriction of printing small part sizes, the studies are made for large scale Additive Manufacturing. Duty et al. [1] mentioned in his study that, although Big Area Additive Manufacturing (BAAM) used the same principle with FDM technology, some differences can be seen to increase the material deposition and enlarge the printed sample sizes. The pellet form of the deposited material is preferred, instead of using filament to decrease the material cost and accelerate the printing speed [2]. Moreover, unlike the pneumatic based deposition systems, screw based polymer deposition is utilized to feed the thermoplastic material, continuously. Hence, big sized parts can be printed with the advantages of providing continuous polymer feeding in the pellet form, which could be resulted in the printing without any interruption. He underlined that, the perfect adjusting of the process parameters and close controlling of the process are needed to accomplish a good printing with minimum voids. Some problems can be seen as a result of the uncontrolled temperature conditions. These problems can be; void or bubble observance, weak bonding and deformations, which can directly affect the parts' mechanical properties and physical appearance.

Post et al. [2] support the point of Duty et al. by stating that, the transition from filament to the pellet is important in the sense of increased performance speed. By using pellet form, melting of the material can be performed more quickly. Post et al. also mentioned that, by printing big sized parts, BAAM technology can use the energy more efficiently. He compared FDM and BAAM technologies based on cost, pre-processing, processing and post-processing time. It was concluded that, BAAM significantly lowers the time of the production and cost. Big sized manufacturing technology can be very beneficial especially in automotive and aerospace areas. Using carbon fiber as a reinforcement by additive manufacturing technique is very critical in the aerospace industry because, compared with heavy aluminium materials, carbon fiber has very light weight properties and in the comparison of molding processes, additive manufacturing can decrease the process time with less cost.

The advantages of the FDM process are as follows; i) having wide area of usage, ii) affordable prices of the machines, iii) suitable alternative for complex shapes and designs, iv) freedom of

design, v) minimum waste and lead time. The disadvantages can be summarized as follows; i) post-processing operations are needed especially in the case of surface finish is critical, ii) long processing times and iii) requirement of good control of the temperature and printing parameters. However, FDM is one of the most promising technology, due to the potential of developing new and reinforced materials, printability of the multi-materials, and improvements in mechanical properties (such as strength and durability). The advantages, disadvantages and limitations of FDM process, is summarized in Table 1.

Advantages	Disadvantages and Limitations
<ul style="list-style-type: none"> • Wide usage area, • Machines with affordable prices, • Suitable alternative for complex shapes and designs, • Freedom of design (huge customisation), • Minimum waste, • Minimum lead time. 	<ul style="list-style-type: none"> • Need of post-processing operations, if surface finish or roughness is critical, • Long processing times, • Need of good control of temperature and printing parameters, • Limited materials and mechanical properties, • Mainly restricted with prototype applications, • Limited with small parts, • Limited sizes of FDM machines.

Table 1 : Advantages, disadvantages and limitations of FDM.

The advantages of the FDM shows the unique characteristics of the process compared with the other technologies. The disadvantages and limitations shows how the technology needs to be improved. The limitations directly restrict the usability of the technology [50]. Hence, improvements are needed to enhance the effectiveness of the process. With the developments on the materials side (such as addition of the new materials and reinforcements, and change the form of the supplied material) and the printing design, mechanical characteristics of the printed parts can be improved and this can increase the application areas and usability of the technology, mainly in the automotive and aerospace industries.

1.3 Materials used in FDM

As mentioned above, thermoplastic materials are commonly used in FDM processes. Thermoplastic materials, normally, are in the solid-state form. But, they have the characteristics of melting and become fluid form, when exposed to the heat. Materials can return to the solid form, in the case of cooling. Some of the thermoplastic materials used in FDM are; Polycaprolactone (PCL), Polylactic acid (PLA), Acrylonitrile Butadiene Styrene (ABS), Polypropylene (PP), Polyetheretherketone (PEEK), ULTEM (polyetherimide), and Nylon [10,17,18, 25]. PLA and ABS are the most commonly used materials in FDM and have been studied extensively [23].

Polylactic acid (PLA) is widely used and biodegradable material which is produced from plant starch. Based on the objective of minimizing environmental foot-print and sustainability principles, PLA is a promising option because of having environmentally friendly properties [13].

Acrylonitrile Butadiene Styrene (ABS) is another commonly used thermoplastic material which has a chemical formula as $(C_8H_8)_x \cdot (C_4H_6)_y \cdot (C_3H_3N)_z$. ABS material has amorphous characteristics and general percent dispersion ranges of Acrylonitrile, Butadiene, and Styrene are; 15-35%, 5-30%, 40-60%, respectively. For ABS; Acrylonitrile has a function of increasing durability and resistance, Butadiene has a function of improving the strength, and finally, Styrene helps to perform improvement on characteristics of processing operation. ABS have prominent features of having good toughness and durability, strong heat and chemical resistance, and performing user-friendly operations. On the other hand, ABS can result in insufficient fatigue strength [40]. One of the studies on ABS by using FDM technology is performed by Naidu et al. [40]. This research investigated the tensile and flexural strength values of the samples which are printed by ABS filament based material. As a result of the study, it is observed that the obtained flexural strength values are larger than the tensile values.

Polycaprolactone (PCL) is a biologically soluble material and indicates high biocompatibility. Thus, it has been extensively studied in biomedical applications. One of the example application areas is in, tissue engineering [15]. PCL's melting temperature is low compared with other materials, which is around 60°C [49]. The materials' flow behaviour is highly dependent on the applied pressure, the design of the nozzle (diameter, shape, and dimensions), and feeding rate. Ramanath et al. [15] investigated on PCL' melt flow behaviour with the FDM technology. The

study is conducted by performing analytical and Finite Element Analysis (FEA) modelling and concluded that totally melt form of the PCL can be obtained with the 42-mm distance interval from the entry point. This study is one of the examples of PCL material usage in FDM printing, with highlighting the importance of obtaining most compatible design depending on the behaviour of the molten material.

Another example study on melt flow behaviour of FDM technology is performed by Sa'ude et al. [16]. Differently, from Ramanath et al. who mainly focused on PLA, this study is analysed and compared flow behaviour of ABS, Polypropylene (PP), Copper and Iron mixed ABS materials. The experiments are conducted by using FEA and ANSYS software and the material flow through the nozzle is taken as a steady-state condition, which means flow properties of the material remain constant with time during the process. As a result of this study, Sa'ude et al. [16] discussed that, ABS mixed with copper and iron resulted in greater performance, compared with unblended materials. This study showed the effect of blending materials and usage of reinforcing materials to obtain better performance.

Polyetheretherketone (PEEK), is a crystalline thermoplastic material that is firstly introduced around 1977, has great mechanical properties, biocompatible characteristics and temperature durability [34,41]. Also, it is a recyclable material with perfectly competing with the strength of the aluminum. PEEK requires high processing temperatures and this could cause difficulties in the heating process [41]. A study about PEEK usage with FDM printing was investigated by Xiaoyong et al. [3]. He stated that, a good adjustment of temperature and filling rate are very critical to achieve desired mechanical properties and strength of the bonds between printed layers. Also, a comparison between PLA and PEEK materials are performed and it is concluded that, PEEK material resulted in greater tensile strength (77 MPa). Depending on the used PLA series, required printing temperature for PLA ranges between 190-230°C. However, PEEK needs greater than 340 °C, which is much higher than PLA. In this study, four different conditions with five tests of each were performed to obtain the results. Different values of the bed and environmental temperature and filling ratio are experimented by using the tensile test based on the standards of ISO 527. According to the test results, an increase in temperature can proportionally affect the strength of the part. It was shown that, with a perfect optimization of the printed parameters and temperature, a better performance on tensile strength can be observed (around 90 MPa, and resulted in 20 percent improvement). This study is effective because of specifying the importance of parameter optimisation which can directly increase the

strength of the printed part, and this is one of the example studies about the performance of the PEEK material, compared to PLA by using FDM technology.

Another study on PEEK material is conducted by Wu et al. [34]. Different from Xiaoyong et al., Wu et al. studied on the comparison between ABS and PEEK materials with the help of tensile and bending test experiments. During the study, the effect of the layer thickness (thickness of the extruded layer) and raster angles (direction of the printed strips) on materials were also investigated. Wu et al. showed that, an increase in the layer thickness, can directly increase the staircase problem which is illustrated in Figure 5. According to the test results, it was shown that, the mechanical performances of PEEK was greater than ABS material (approximately 100% enhancement). Also, Rahman et al. [41] analysed the mechanical testing of PEEK material (tensile, flexural and impact testing) with various raster orientations. As a conclusion of this research, 0° raster orientation gave the greatest ultimate tensile strength values. For flexural strength; 0° raster orientation resulted in the largest modulus of rupture.

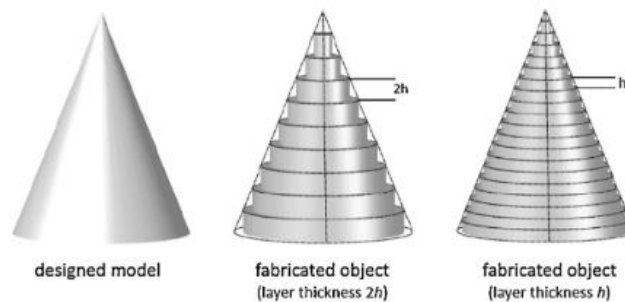


Figure 5: Representation of staircase effect based on layer thickness [44].

ULTEM is another alternative material can be used in FDM based 3D printing. One of the widely used ULTEM material types is ULTEM 9085. In addition to ULTEM 9085, ULTEM 1000 is also used and requires greater glass transition temperature (T_g) than ULTEM 9085 [22]. Chuang et al. [22] reported a comparative study with the usage of ULTEM 9085, ULTEM 1000 with reinforcement of chopped carbon fibers, as feeding materials in FDM technology. The results from this study showed that, based on the mechanical test, drying process applied ULTEM 1000 with chopped carbon fiber reinforcement showed improvements in a tensile test.

Determining the optimal temperature for the printed material, is very effective to increase the performance of the printing. As an example, Sukindar et al. [8] studied on PLA materials' optimum temperatures with the help of flow analysis on ANSYS program. According to the study, it was concluded that, the optimal temperature value for PLA can be 190°C . In this study, it was shown that, the determination of best-fit temperature value for the used printing

material can have a key role to perform good printing. Also, Lindberg et al. [27] stated in his study that the process temperature has a significant impact on the materials characteristics.

Also, the printed parts adhesion to the platform can be varied, depending on the printing material. The adhesion between the printed material and the printing bed is very critical because, it had a direct effect on the surface roughness of the parts, appearance and easy separation from the bed, after the process completed. A tight adhesion can result in the deformation of the part and even the breakages can be formed. On the other hand, a light adhesion cannot be durable to the printing process and inadequate traction forces may result in irregular printing. Thus, depending on the material used, a most compatible type of the print bed need to be selected. As an example; Carneiro et al. [17] discussed that, using polypropylene (PP) as an extrusion material, is not very compatible with the commonly used printing surfaces. Hence, pre-processing techniques are required to ensure a good adhesion between the material and the bed. Similar with the goal of achieving optimal adhesion, an improved surface roughness can be obtained by using post-processing techniques. Post-processing methods are highly dependent on the material used. As an example, Fernandez et al. [21] investigated economical chemical post-processing method and their effects on impeller parts which are printed by using an FDM technology. Acetone and bath dipping are some examples of chemically improved methods for the printed part. Depending on various studies, post-processing techniques can result in an increase of the performance. Agarwala et al. [32] showed that, post-processing methods can be used to mitigate the surface problems of the printed part. However, he noted that, post-processing method cannot be beneficial, in the case of fabrication of the internal features.

For achieving better mechanical performances, drying of the material could be used. Depending on the material used, the drying procedure and its processing time can vary. As one of the example; Chuang et al. [22], reported that, the drying process of the supplied filaments can be important, because of the effect of improving parts performance. The drying process is taken place in the oven at 185°C and the processing time is approximately 12 hours. Drying procedure is important because, printing materials can become more robust and durable with resulting lesser porosity between the bonds of the material. Moreover, depending on material used, the printing parameters (such as temperature, required pressure, and feed rate) optimization is required to obtain successfully printed samples with FDM technology [14].

Additionally, investigation of the feed rate and the determination of the optimum value is important, for consistent material flow during printing. Ibrahim et al. [19] reported a study related to the effect of the feed rate by using ABS, High Impact Polystyrene (HIPS) and ABS-Copper materials. He pointed out that, very high feed rate speed can result in undesired errors and detriments. On the other hand, increase in the feed rate, can shorten the printing process time. So, there exists a threshold between deciding on the optimum feed rate, which is also related to the materials used. Moreover, the processing temperature has a significant impact on the printing parts' quality and flow of the material.

As shortcomings; it is important to note that, many studies are conducted based on the pure thermoplastic polymer FDM printing. Parallel with the recent developments, and the need of mechanically stronger and durable parts to broaden the application areas of AM, pure thermoplastic polymers could be inadequate. With the addition of the fiber reinforcements to the thermoplastic polymers, the printed parts could meet demanding needs. In other words; composite printing, which is the printing of the material, that has a combined structure of at least two materials, can be used to increase the mechanical performance and the usability of the printed parts. Hence, lately, investigations on the printing polymers with the reinforcement materials (like carbon fibers) has been increasing [46].

1.4 Reinforced materials in FDM

Usually, fiber can be found in several types, which are; Glass, Kevlar, Natural jute, and Carbon fiber. Carbon and glass fibers are the most commonly used fiber types. Melenka et al. [12] investigated the mechanical tests of the reinforcement of Kevlar fiber with Nylon material, by using FDM technology. As a result of his study, it was concluded that printing materials' reinforcement with fibers had a promoting effect on the elastic modulus. In addition, an enhancement in strain and stiffness values can be observed with the usage of fiber. As a problem mentioned in the study; a fluctuation of the fibers could be observed, which is caused because of the adhesion and non-uniform or inadequate pulling force of the fibers. The fiber fluctuation can result in a decrease of the mechanical performance, and a reduction in the printing quality. This study also highlighted the importance of analysing the fibers' start point locations on the sample, which could be resulted in a great intensity of stress, and may lead to undesired failures.

Natural jute fiber is a plant based fiber which is the perfect candidate for recyclable printing processes [37].

Bettini et al. [47] studied continuous aramid fiber implementation with PLA material. It was pointed out that, slow deposition rate is recommended to achieve maximum control of the printed sample. Mechanical tests are performed to observe the effect of using continuous aramid fiber. According to the obtained results, it was concluded that fiber reinforcement can increase the strength of the printed parts.

As an example study with reinforcing glass fiber, Carneiro et al. [17] analysed pure and reinforced glass fiber (30%) polypropylene (PP) to compare mechanical performances. Based on the conducted tests, the glass fiber reinforced polypropylene resulted in greater values, compared to the pure PP.

The reinforced fiber materials in the FDM can be categorized into three, based on the implemented form and the length of the material. These are; chopped (short) fiber, nano-fiber and continuous (long) carbon fiber. FDM technique can be utilized for implementing the both, chopped and continuous fiber. Also, carbon fiber has the characteristics of being electrical conductive [55].

Prüß et al. [4] studied on printing with fiber reinforcement which can increase the mechanical characteristics of the printed parts. In this study, Prüß et al. [4] stated that, a short form of fiber reinforcement can be achievable with some of the additive manufacturing techniques like FDM, SLS (Selective Laser Sintering) and SLM (Selective Laser Melting). However, FDM is the important method which can utilize the continuous fiber as reinforcement, and the adjustment of the fiber orientation can be controlled. To be able to use continuous carbon fiber, modifications needs to be done in the machine design, to achieve the optimal printing. The improvements on the process design can improve surface roughness, minimize the problems due to the staircase effect, which is dependent on the layer thickness, minimize the warpage and curvature effect, and maximize the mechanical properties. Using carbon fiber can prevent the warpage of the printed part, which is the main problem for printing large and flat parts. An important study performed by Prüß et al. [4] showed the importance of the using continuous carbon fiber, and how fiber reinforcement could increase the mechanical properties with minimizing the warpage.

Similarly, Ning et al. [10] studied on carbon fiber reinforced FDM printing and analysed carbon fiber reinforcement effects on the printed parts' mechanical performance, by using tensile and flexural tests. For this experiment, pellet form of ABS and powder form of carbon fiber are used as printing materials, and blending is performed with various contents of carbon fiber to generate deposited filament. After the tensile and flexural test, it was concluded that adding carbon fiber can increase the tensile strength and improve the mechanical properties of the printed part.

Girdis et al. [20] reported in his study that, up to 22% enhancement of the tensile strength could be achieved with the addition of 2 wt% (weight percent) chopped fiber, as a reinforcement to the printing material. As underlined from this study, even a small amount of chopped fiber addition, can have a potential to increase the mechanical properties of the printed samples. Another study on chopped fiber involved ABS material was performed by Tekinalp et al. [43]. Different chopped fiber percentages (none/10/20/30/40wt %) were used to investigate the effect of the fiber rate on the mechanical properties. The results showed that an enhancement was observed in tensile strength and modulus by using chopped fiber as a reinforcement material. However, due to using fibers, voids are observed in the printed samples which have a direct effect on lowering the mechanical properties. Apart from the void formation, adding fibers caused weak adhesions between the layers and stripes. Also, he reported that breakage of the fiber can result in a huge decrease in the mechanical properties.

Thus, adding reinforcing fibers could increase the mechanical properties of the samples. The 10 wt% carbon nano-fiber addition as a reinforcement into the thermoplastic polymer, could result in 39% improvement in the tensile strength values [46]. Also, for the chopped carbon fiber, the addition of 5 wt% chopped fiber could result in approximately 42 MPa tensile strength value [10]. Compared with the both, chopped and carbon nanotube (CNT) fiber reinforcements, continuous carbon fiber reinforcement has higher mechanical improvements [5,6].

1.4.1 Continuous carbon fiber reinforced material in FDM

One of the important studies on continuous carbon fiber printing with thermoplastic materials, was developed by van der Klift, et al. [36]. This study aimed to investigate the effect of carbon fiber reinforced thermoplastic (CFRTP) materials by conducting tensile tests. Nylon and continuous carbon fiber (1K) are used and printed samples had 10 number of layers. Three

distinct types of samples are printed which are; pure nylon (10 layers of pure nylon, no fiber inclusion), 2 layers of nylon in sides with 6 layers carbon fiber in middle, and finally, 4 layers of nylon located on the sides with 2 layers carbon fiber in middle samples. Experimenting with three distinct types of samples is important because, it could show the benefit of using carbon fiber and the effect of including more fiber volume. In this study, it was reported that using continuous carbon fiber greatly increased the obtained tensile values. However, van der Klift, et al [36] noted that, because using carbon fiber could cause void formations, the sample that had 6 layers of fiber, resulted in larger voids compared with the 2-layered fiber sample, which is presented in Figure 6.

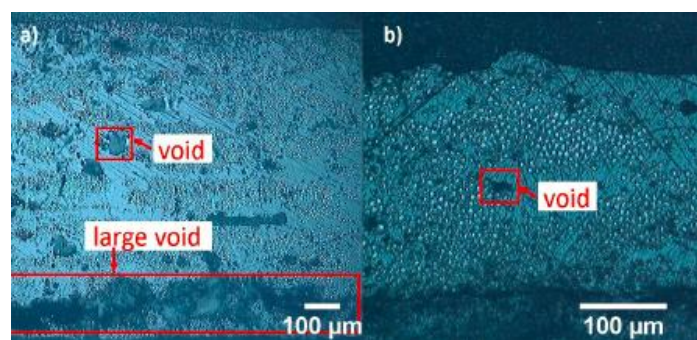


Figure 6: Cross section views of the 6-layered carbon fiber (left) and 2-layered carbon fiber (right) [36].

Additionally, fiber distribution and continuity during printing is very critical, to achieve the desired outcomes. Another significant study about continuous carbon fiber composite printing, was developed by Matsuzaki et al. [37]. Continuous carbon fiber filament and filament form of the PLA, are used, and materials are fed into the nozzle individually. Feeding mechanisms of the materials can be seen in detail in Figure 7. The experiments are conducted based on the samples printed with pure PLA, carbon fiber reinforced thermoplastics (CFRTP) and jute fiber reinforced thermoplastics (JFRTP). So, this study did not only investigate the effect of carbon fiber, but also the carbon and jute fiber. The tensile modulus and the tensile strength comparison bar-chart graphs from this study can be seen in Figure 8. Depending on the results, it could be stated that, in both tensile modulus and strength tests, carbon fiber reinforced thermoplastics gave strongly larger values in the comparison of pure PLA (approximately over 400%-500% higher results). Moreover, Matsuzaki et al. [37] agreed on the point that van der Klift, et al. [36] stated that using carbon fiber could highly increase void formation, which is one of the frequent problem in FDM based techniques.

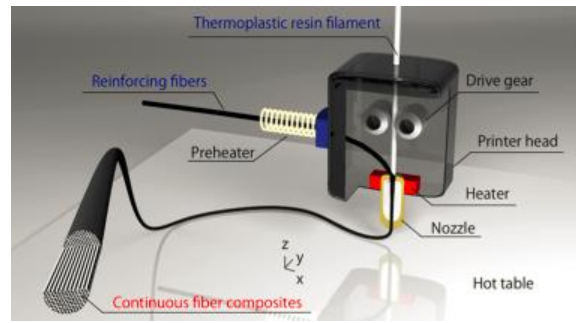


Figure 7: Feeding mechanism of the materials; PLA (top) and continuous carbon fiber (side) [37].

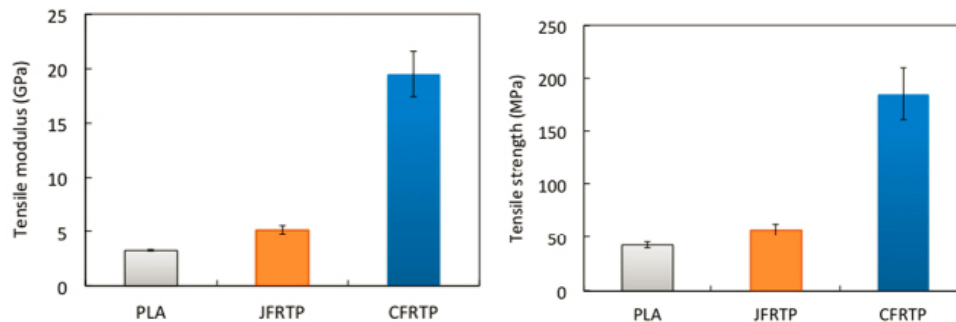


Figure 8: Tensile modulus (left) and tensile strength (right) comparisons of PLA, JFRTP and CFRTP [37].

As a pioneering work of the study of Matsuzaki et al. [37], continuous carbon fiber based on FDM technology was developed by Namiki et al. [39]. As similar to Matsuzaki et al., continuous carbon fiber (1K) and PLA are used and fed into a nozzle. The nozzle diameter is determined as 1.4 mm, which is larger compared with the commonly used FDM nozzle, to decrease the risk of having clogging. A sample dog-bone shape is printed (Figure 9) and the tensile tests were performed. As a result, carbon fiber reinforced PLA showed better tensile modulus values compared with the pure PLA samples. On the other hand, it was observed that due to the carbon fibers' properties, the printed carbon fiber could not perfectly embedded into the PLA material. In other words, carbon fiber cannot be totally centralized in PLA; instead, carbon fiber located much towards to the surface of the printed samples. This study pointed out the problematic sides of embedding the carbon fiber during printing, such as; positioning carbon fiber in the middle of the printed samples and unable to achieve perfect sinking in the printed material.

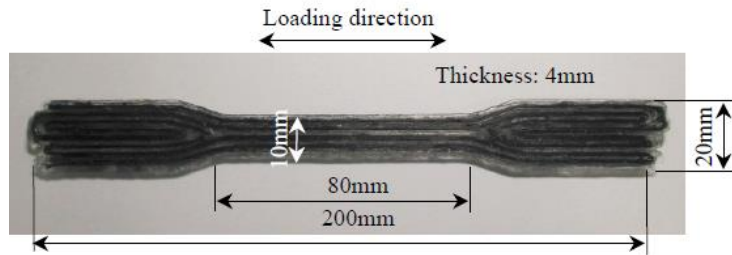


Figure 9: Printed sample with carbon fiber reinforced PLA material [39].

Additive manufacturing of carbon fiber and PLA using FDM was also analysed by Bade et al. [38]. According to this study, carbon fiber included and pure PLA samples were printed and the tensile tests were conducted. The printed filament of carbon fiber embedded in PLA material and their dimensions can be seen in Figure 10. Similar to the other studies, it was concluded that reinforcing PLA with carbon fiber result in a greater tensile strength. In addition, it was shown that the dispersion of the fiber is very important which can have a direct impact on the mechanical performance of the printed samples.

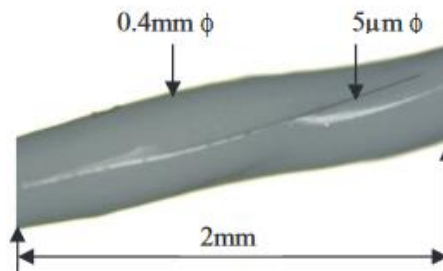


Figure 10: Printed carbon fiber and PLA filament with their dimensions [38].

Another recent study was conducted by Nakagawa et al. [51] and in this study, carbon fiber was used as a sandwich structure with ABS material by the application of fused deposition modelling technique. In other words, carbon fiber is located in the middle of the base and top layers. Carbon fiber and ABS filaments are supplied together from the same part of the single nozzle. ABS filament with a diameter of 1.75 mm and 9000 carbon fibers with certain lengths, were used for forming of the sandwich structure. According to the tensile test, it was stated that; carbon fiber inclusion as a sandwich form could increase the strength of the printed parts. However, the addition of thermal bonding processes had a great impact on the strength value, due to the enhancement of bonding between the deposited layers. In the absence of the process of thermal bonding, it was reported that slippage of carbon fibers were observed and mechanical

test analysis could not be perfectly determined. Mechanically tested samples with the addition and lack of thermal bonding, can be seen in Figure 11.

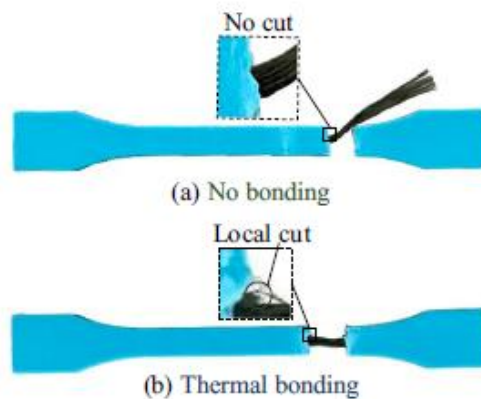


Figure 11: Samples without (upper) and addition (lower) of the thermal bonding process [51].

Thermal bonding was performed by using a microwave oven at 270W about 20 seconds. Also, as another alternative, the heating pin could be used to achieve the sectional heating. However, compared to microwave oven, this application method could be exhaustive and time-consuming. Hence, using a microwave oven could be an optimal solution. As a result of the mechanical tests, it was pointed out that with the addition of the thermal bonding process, the samples' strength values were improved. It was an important study because, the implementation of thermal bonding as a post-processing technique, could have a supportive effect on improving mechanical test results of the printed samples. Moreover, it has suggested that, bonding between polymer and carbon fibers bonding could become stronger by using boron nitride.

Tian et al. [5] published a study on continuous carbon fiber and PLA in an FDM process. 1K carbon fiber bundle and PLA filament were used, and by comparing flexural strength test results, the temperature and pressure effect on process parameters (layer thickness, feed rate, hatch spacing) were investigated. It was concluded that, the optimal values for temperature, layer thickness, and hatch spacing were 200-230°C, 0.4-0.6 mm and, 0.6 mm, respectively. Also, the optimal fiber content determined as 27% that could result in the highest flexural strength. The bonding of layers can be enhanced with an increase of the pressure, and strong bonding directly influences printed parts mechanical properties. This study underlined the effect of the temperature and pressure on the printed parts. Moreover, it was reported that, shifting (slipping) of fiber was one of the observed problems during the printing process.

Fiber slipping, which is the decentralization of the fiber, can be one of the main problems occurred with the usage of continuous carbon fiber in FDM technique. The continuous form of

the fiber tend to slip sideways and these conditions create decentralization. The decentralization of the fiber can highly influence the printing and can decrease the performance and mechanical properties of the printed parts. Minimizing the slipping effect and perfectly centralization of fiber can result in a greater mechanical performance.

The bonding between layers and implemented materials has a direct effect on increasing parts' quality. To increase the bonding force of the carbon fiber and thermoplastic polymer, some additional operations could be performed to modify the carbon fiber. As an example, Li et al. [11] mentioned in this study that, the carbon fiber filament modified with using methylene dichloride and the filtration process; the printed samples with modified carbon fibers resulted in higher strength values compared with the pure PLA and unmodified carbon fiber-PLA samples. When unmodified carbon fiber reinforced PLA and pure PLA compared, approximately 186% and 12% improvements were observed during tensile and flexural tests respectively. These improvement values were highly increased, when modified carbon fiber reinforced PLA samples were used. This study was a good example to show how modifications could affect the strength of the materials and resulting in better bonding.

Die swelling, which is the dilation condition of the melted polymer during the printing, is one of the widely observed phenomenon on the extrusion based methods. The amount of the die swelling is hugely depended on the material used and the shape of the designed nozzle. The die swelling illustration can be seen in Figure 12. According to Turner et al. [31], using carbon fiber could help to decrease the probability of die swelling.

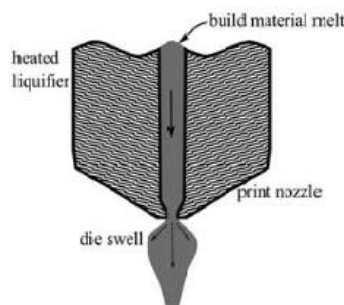


Figure 12: Presentation of die swelling [31].

Advantages of using carbon fiber as a reinforcement material are summarized in Table 2.

Advantages of Carbon Fiber Reinforcement
<ul style="list-style-type: none"> • Minimize the warpage effect
<ul style="list-style-type: none"> • Strong bridging capability, minimize the need of support structure and improve overhangs
<ul style="list-style-type: none"> • Improvement in mechanical properties (locally and globally)
<ul style="list-style-type: none"> • Having lightweight property
<ul style="list-style-type: none"> • Recyclable

Table 2: Advantages of using carbon fiber as a reinforcement [4,5,9,10,26,29,48].

1.4.2 Problems on continuous carbon fiber

Besides the great advantages of using carbon fiber as a reinforcement, some problems can be observed with the addition of continuous carbon fiber. As stated previously, slippage and fluctuation of fibers could affect the quality of the printing. Due to the fibers' rigid characteristics, breakages could happen very easily. The formation of the breakages could negatively affect the mechanical performance of the printed parts. Moreover, some adhesion problems may have observed between the deposited layers, with the addition of the continuous carbon fiber. Importantly, one of the most encountered problems with the usage of continuous carbon fiber is void formation. As van der Klift, et al. [36] and Matsuzaki et al. [37] mentioned, using continuous carbon fiber could trigger the formation of voids. Also, as Namiki et al. [39] supported that, during the printing process, continuous carbon fiber cannot be totally centralized and embedded. Because continuous carbon fiber has very fragile structure, during the deposition and printing, undesired agglomerations can be formed, which can result in nozzle clogging [44]. This case could be observed especially with the small nozzle diameters.

Nozzle diameter is an important parameter which influences the parts quality, processing time and surface roughness. Sukindar et al. [13] studied on the various nozzle diameters (range of 0.2-0.4 mm) and mentioned in his study that, the small diameter of the nozzle can lead increase in accuracy. Moreover, processing time is highly dependent on the nozzle diameter. Increase in the nozzle diameter, accelerates the printing and decrease the processing time. Sukindar et al. pointed out this issue and stated that optimization is required to balance between the process time and the accuracy. Shorter processing times and better accuracy are desired to obtain parts that have superior performances.

Using larger nozzle helps to reduce the risk of having clogging. Clogging caused by materials or heating problems can result in the inconsistency during the printing. Consequently, the part can have undesired defects, voids and over or insufficient materials may be observed [27,37]. As an example, Girdis et al. [20] mentioned the clogging problem experienced during his study and noted that; due to the nozzle clogging, printings need to be repeated numerous times and this resulted in material waste and over workforce. As a drawback of using larger nozzle; the resolution of the printing may not be good and this could directly affect the quality and the performance of the printing [39].

An optimal nozzle design is critical to have successful printing for a better bonding between layers, minimum voids and superior quality. In the study of Zemcik et al. [7], two different printer head designs were compared using ANSYS program. As a result, it was concluded that, increasing the length of the melting chamber in the design can have a negative effect on the quality of the printed part, and this can directly result in deterioration in part quality.

The problems with using continuous carbon fiber are summarized in Table 3.

Problems with using continuous carbon fiber
<ul style="list-style-type: none"> • Fiber slipping (decentralized fiber location), undulation of the fiber
<ul style="list-style-type: none"> • Fiber breakage
<ul style="list-style-type: none"> • Adhesion problems (weak adhesion)
<ul style="list-style-type: none"> • Void observation
<ul style="list-style-type: none"> • Cannot be perfectly embedded into the printed material
<ul style="list-style-type: none"> • Increased chance of having nozzle clogging (especially with the small nozzle diameters)

Table 3: Problems with using continuous carbon fiber [5,6,11,12,36,37,39,44].

1.5 Coaxial Printing

Coaxial printing is a recent technique where more than one materials are printed separately in a common axis. Materials are fed and melted separately and the supplied materials come together and merged to achieve a concentric printing by using one common axis. Coaxial printing has a cross-sectional area of two different regions of circles. These are; internal

(centered or core) and external (off-centered or shell) material deposited areas, as seen in Figure 13. Compared with the standard FDM printing, coaxial printing requires higher complexity in the nozzle design and good control of the process. Thus, investigations on this subject are very limited [30].

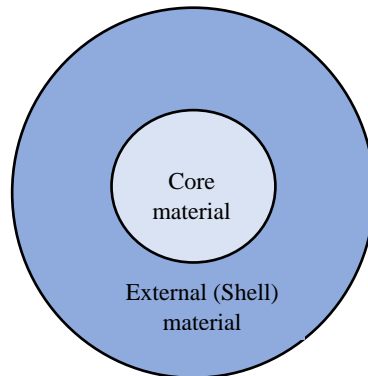


Figure 13: The cross-section area of coaxial printing, internal and external material, top view [30].

One of the recent studies on coaxial printing was conducted by Taylor et al. [30]. For this study, filament form of PLA and ABS are selected as separately supplied materials, and new coaxial nozzle design was developed. Also, this study focused on analysing the concentricity of the internal and external materials. White and purple coloured PLA materials were used and a simple extrusion was performed. In other words, 3D printing wasn't performed due to the elimination of the traction forces, which can have an effect of sliding the internal and external areas. As a result, it was concluded that; an increase in the concentricity of the materials can be achieved by controlling the viscosity of the supplied materials and finding an optimum process temperature. Hence, optimization of printing parameters for determining optimal temperature and feed rate was needed, to obtain better concentric printings. This study is an example study on performing coaxial printing and mainly concentricity of the materials were investigated. However, as a shortcoming, this study did not use carbon fiber as a reinforcement.

1.6 Objectives for this project

This thesis aims to develop an FDM based coaxial additive manufacturing of continuous carbon fiber reinforced thermoplastic (PLA) composite materials. The motivation behind the project is to improve the mechanical performance of the 3D printed samples compared to pure PLA. Because there have been very limited studies on the coaxial printing, this thesis work is one of

the pioneering studies on the coaxial continuous carbon fiber printing and comparative mechanical tests of the continuous carbon fiber reinforced and pure thermoplastics. This projects first objective is to develop a coaxial nozzle to perform continuous carbon fiber reinforced composite 3D printing, and investigate the effect of including continuous carbon fiber as a reinforcement in thermoplastic PLA polymer matrix material. Moreover, the adhesion of continuous carbon fiber and penetration in PLA, is analysed. After the printing of the samples, tensile and flexural (3-point bending) tests are conducted and obtained data is analysed for carbon fiber reinforced and pure PLA conditions, individually. Also, the printing parameters such as temperature, pressure and feed rate are studied to determine optimum values.

2. EXPERIMENTAL DESIGN & METHODOLOGY

2.1 Overview of the Methodology

The overall steps performed in this thesis are represented in Figure 14. Designing and manufacturing of the coaxial nozzle were the initial part of the thesis work. Then, materials (continuous carbon fiber as reinforcement and thermoplastic polymer) and equipment were prepared. By using the developed setup, the 3D printing process was performed. Then, the mechanical tests were used to investigate the effect of using continuous carbon fiber on the printed samples. For mechanical analysis, the tensile and flexural tests were performed with the implementation of predefined standards and methods by ASTM (American Society for Testing and Materials). Continuous carbon fiber and pure polymer 3D printing were performed to be able to compare their mechanical test results. As a final stage, obtained data from the conducted tests were analysed and concluded.

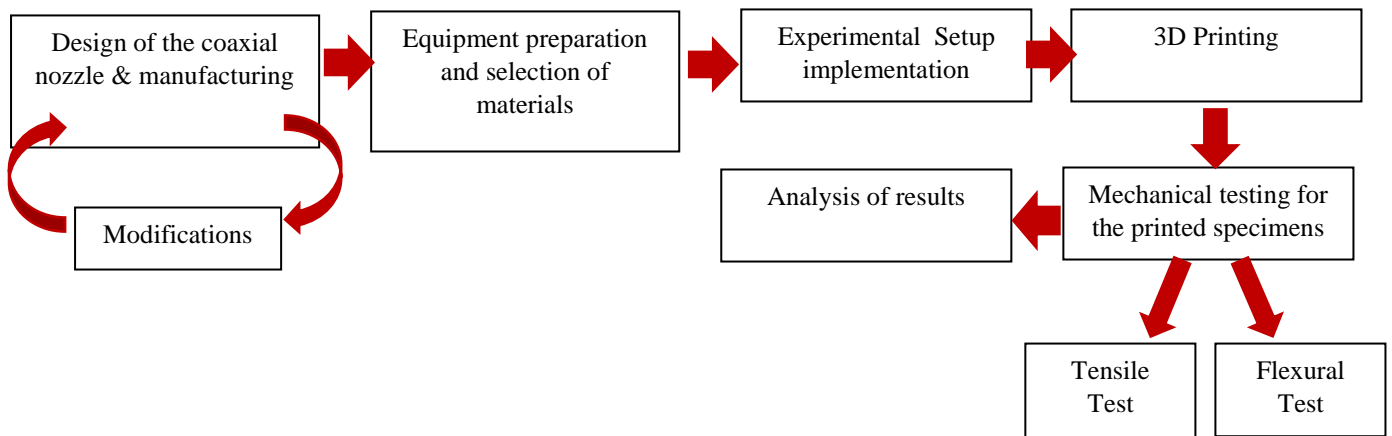


Figure 14: Overview of the conducted methodology.

2.2 Design and development of the coaxial nozzle

2.2.1 Design for the carbon fiber reinforced thermoplastic printing

As the first step in this thesis, nozzle design is needed to be developed for performing coaxial printing. Before the initial design, current FDM nozzle designs were investigated and possible scenarios were generated. Different nozzles were designed by using SolidWorks software. Based on the drawings from SolidWorks, the components of the nozzle were manufactured in the Sabancı University Machine Shop by using the machining techniques. The material used for manufactured parts is Aluminum-6000 series. After the initial design development and manufacturing, modifications were made for improving the functionality and performance of the design. For the coaxial design, the main goal is supplying the continuous carbon fiber and thermoplastic polymer material separately, and performing their well-integration inside of the nozzle, before the printing.

After the design in SolidWorks, parts are manufactured separately. The design of the nozzle contains 3 main components. Parts were fastened with each other to provide assembly of the nozzle. The feeder is used for supplying continuous reinforcing fiber. The polymer syringe is used for supplying the thermoplastic polymer in pellet form. Thermoplastic polymer needs to be heated in this aluminum syringe and then injected to the liquefier. Also, syringe cap is manufactured, and need to be tightly connected to the polymer syringe, to connect to the air supply. The liquefier had a connection between both the continuous carbon fiber feeder and the

polymer syringe. This part had a function as integrating and combining materials, so coaxial printing can be performed. Also, the liquefier has holes for the cartridge heater and thermistor. Nozzle tip had the diameter of 2.5 mm. The initial design of the coaxial nozzle with individually manufactured 3 main components and cap, can be seen in Figure 15.

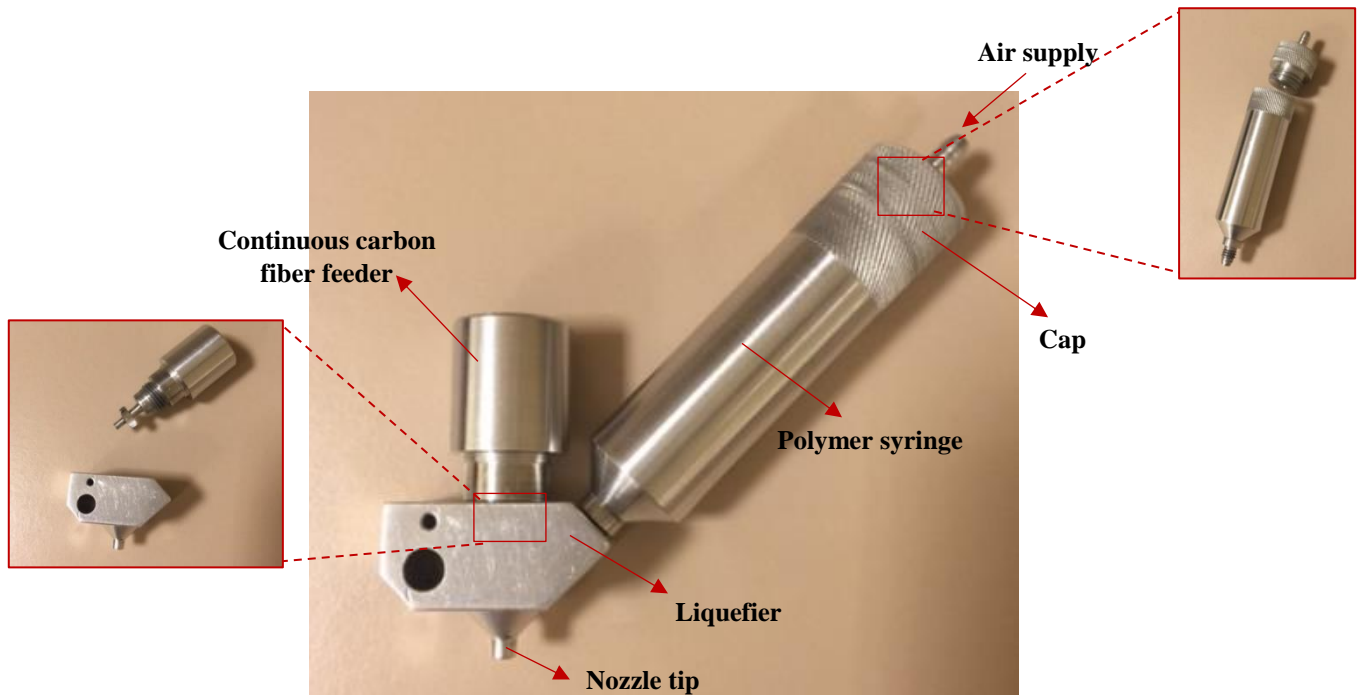


Figure 15: The initial design of the coaxial nozzle with 3 components and cap, fully assembled view.

The continuous carbon fiber feeder had an additional partitioned design, which had a function to provide a controlled flow of the molten thermoplastic polymer from the syringe through the liquefier. In addition of the manufactured parts, an end-cap was also manufactured by using the same material (Aluminum), which has a screw to fasten and hold the polymer syringe in the perpendicular position. Fixing of the syringe can be needed in the case of addition of thermoplastic polymers to melt, and it can be put inside of the vacuum oven so drying process can be performed.

Modifications were made and parts were manufactured with the same material. An enlarged polymer syringe design, which have a greater capacity of containing polymer pellets compared with the initial design, is designed in SolidWorks and part is manufactured. By enlarging the syringe, 3D printing of the larger specimens could be achieved. Additionally, continuous carbon fiber parts' height was increased, and by having the longer piece, continuous carbon fiber could

be located closer to the center, which is more desired during printing. With the increase of the height, carbon fiber could have more chance to adjust its position and perform sliding towards to the center. The final design is shown in Figure 16.

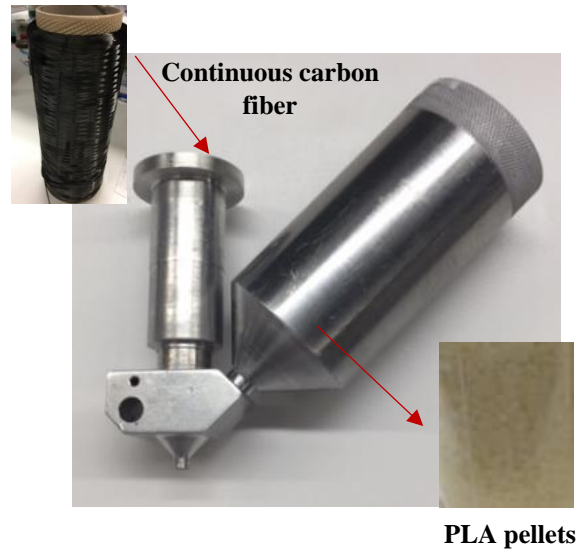


Figure 16: Final design of the nozzle.

2.2.2 Design modification for pure PLA printing

For printing pure PLA, the continuous carbon fiber feeder needs to be changed due to hollow shape of the part. The hollow feature of the original feeder design can affect the quality of the printing with the pure PLA, and voids can be observed between the deposited layers. Hence, new part needs to be designed in order to successfully print with pure PLA for comparing the mechanical test results obtained from printing the reinforced and pure PLA. The newly manufactured part for the pure PLA have almost the same design with the carbon fiber part with a solid inside. By having this design, pressure could be directly applied to the molten material and printing could be successfully performed.

The modified and manufactured design for the pure PLA and the comparison view of the coaxial printing with carbon fiber and pure PLA designs can be seen in Figure 17 and 18, respectively.

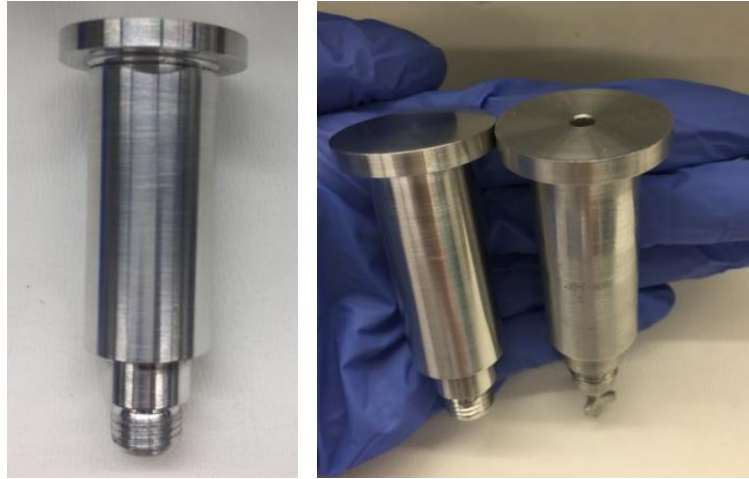




Figure 17: Manufactured part for printing pure PLA , Figure 18: Design comparisons for pure PLA (left) and continuous carbon fiber (right).


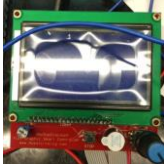
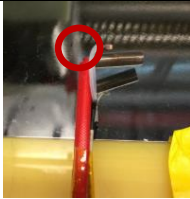






2.3 Equipment used and materials

The electrical and mechanical equipment and materials are used to perform setup implementation and experimentation of the 3D printing.

2.3.1 Electrical and mechanical equipment

The electro-mechanical components used are specified and explained in Table 4.

Equipment	Explanation	Image Representation
Arduino Board (Arduino Mega 2560)	It is a connected board with Ramps 1.4 and Marlin software is utilized to have communication with the Arduino board. (Robotistan)	
Marlin Firmware	It is an essential software to communicate with the Arduino Board. Required changes need to be done in Marlin software's code and coupling with the Arduino need to be achieved. Then, the modified code is uploaded from the computer to the Arduino.	

Ramps 1.4 Shield	Ramps 1.4 functions as taking Arduino's signals and with the wire connection exist on top of the board, thermistor, cartridge heater, and power supply communications can be connected. (Yeşilköy Elektronik)	
LCD Controller	It functions as a display unit of setting parameters such as; temperature of the nozzle and fan. (Yeşilköy Elektronik)	
Thermistor (100K)	It controls and equilibrates the temperature distribution of the nozzle and keep the system at constant temperature which is set from the Arduino Board. (Robotistan)	
Cartridge Heater (12V 40W)	With cartridge heater, heating of the nozzle is performed. Control of the cartridge heater is done by using Arduino Board and screen [14]. (Robotistan)	
Heat Jacket	It is responsible of heating the polymer syringe part. Its maximum heating temperature is 185°C.	
Teflon hose and metal connector	It is a hose from the syringe cap and Nordson EFD, to exert and transmit the pressure from the pneumatic system. Material of it as selected as Teflon, for higher processing temperatures.	
Power Supply	It is a main power of the system and it has direct connection with sockets. (Yeşilköy Elektronik)	
Nordson EFD air controller	It is the pneumatic system used to perform material deposition in the 3D printing. Maximum pressure value which can be set is 5 bars. (Nordson)	
Wiring Kit	It is utilized for the connection operations between power supply and other electrical equipment. (Robotistan)	


Teflon Nozzle and Syringe Holder	<p>It is important to hold the nozzle constant during printing, part connected with platform and syringe to perform the printing. Teflon is chosen due to its non-dispersive property of heat. Using metal or aluminium can result in heat distribution and system cannot be heated to the desired temperature because of the heat loss.</p>	
----------------------------------	--	---

Table 4: Electro-mechanical components of the system.

2.3.2 Materials

Continuous carbon fiber as a reinforcement material and PCL 6400-6500, and PLA 4043D were used as thermoplastic polymer matrix materials, for 3D printing.

2.3.2.1 Continuous Carbon Fiber

For the reinforcement material, 3K (3000) continuous carbon fiber bundle is purchased from Dowaksa Aksaca Ileri Kompozit Mal. San. Ltd Sti. The 3K continuous carbon fiber's technical data sheet is given in Figure 19.

FIBER PROPERTIES

	English		Metric		Test Method
Tensile Strength	552	ksi	3800	MPa	ISO 10618
Tensile Modulus	34,8	Msi	240	GPa	ISO 10618
Strain	1,6	%	1,6	%	ISO 10618
Density	0,064	lbs/in ³	1,78	g/cm ³	ISO 10119
Yield	7,448	ft/lbs	200	g/1000m	ISO 1889
Sizing Type & Amount	D012		1,0-1,5	%	ISO 10548
Twist	Never twisted				

PACKAGING

The table below summarizes the standard packaging; other bobbin sizes can be supplied to satisfy special needs.

Tow Sizes	Bobbin Net Weight (kg)	Bobbin Size (mm)					Spools per Case	Case Net Weight (kg)
		a	b	c	d	e		
3K	1	76	83	280	110	250	12	12

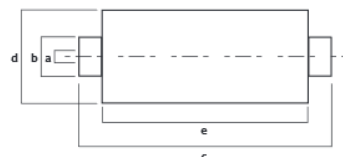


Figure 19: Technical data sheet of the Continuous Carbon Fiber 3K A-38, supplied from AKSACA [52].

To investigate the diameter and the view of the continuous carbon fiber, the SEM images were taken. The measurements were taken from various points and sections of the carbon fiber to obtain more accurate results. By taking the average of these values, the fiber diameter was calculated as 5,77 micrometer (μm), as shown in Figure 20.

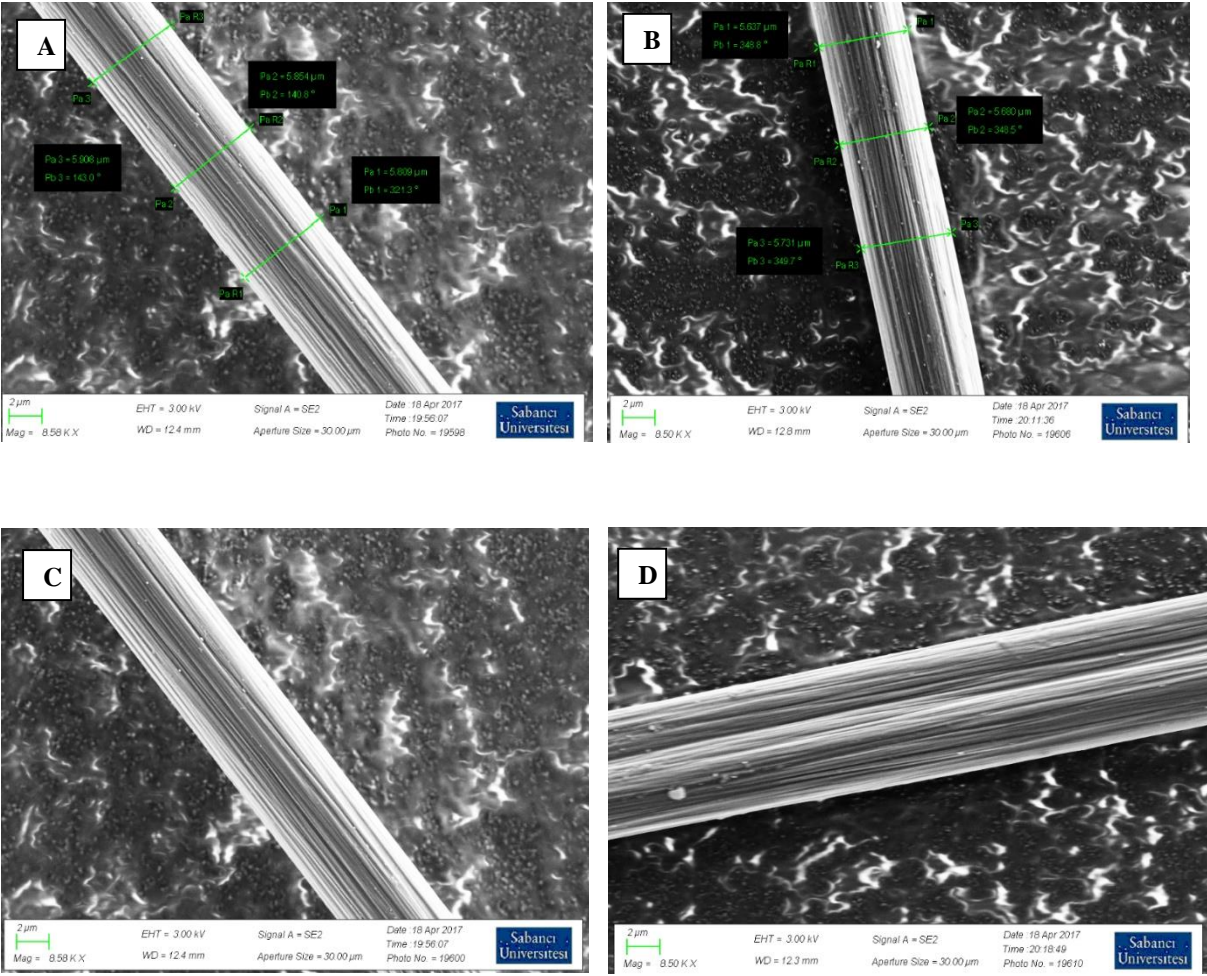


Figure 20: SEM images of continuous carbon fiber. (A) and (B) presents the obtained measurements, (C) and (D) presents single and two carbon fiber views, respectively.

Also, with using Nikon Eclipse ME600 optic microscope, the continuous carbon fiber is examined and the diameter of the fiber was measured as around 5 μm , with 20X magnification.

2.3.2.2 PLA 4043D

After initial trails performed with PCL, which has a low melting temperatures (around 60°C), PLA 4043D pellet form was used as 3D printing thermoplastic material. PLA 4043D was used as the matrix material for printing the samples. Before the direct implementation of PLA 4043D in the printing, PLA pellets were placed in a vacuum oven for 6 hours at 47°C for removing any moisture content inside the polymer for better printing. A BINDER vacuum oven was used in this process and it has the maximum operating temperature of 200°C. Depending on the vacuum oven used, the processing time could increase (or decrease). After the vacuuming procedure, the dried PLA material kept in a desiccator. Figure 21 gives the technical data sheet of the PLA 4043D thermoplastic polymer.

Film Properties		Ingeo 4043D	ASTM Method
Density		1.24 g/cc	D1505
Tensile Strength	MD	16 kpsi	D882
	TD	21 kpsi	D882
Tensile Modulus	MD	480 kpsi	D882
	TD	560 kpsi	D882
Elongation at Break	MD	160%	D882
	TD	100%	D882
Elmendorf Tear	MD	15 g/mil	D1922
	TD	13 g/mil	D1922
Spencer Impact		2.5 joules	
Transmission Rates	Oxygen	675 cc-mil/ m ² -24hr-atm	D1434
	Carbon Dioxide	2,850 cc-mil/ m ² -24hr-atm	Internal
	Water Vapor	375 g-mil/ m ² -24hr	F1249
Optical Characteristics	Haze	2.1%	D1003
	Gloss, 20°	90	D1003
Thermal Characteristics	Melting Point	145-160°C	D3418

Figure 21: Technical data sheet of the PLA 4043D pellets, supplied from NatureWorks LLC. MD: machine direction and TD: transverse direction [58].

2.4 Experimental Setup & 3D printing

2.4.1 Experimental Setup and procedure

After the designed parts were machined and produced, the connections of the electrical and mechanical components need to be made. The Ramps 1.4 board on the top of the Arduino and all the cartridge heater, thermistor, LCD controller, and power supply were connected by using

wiring kit on the Ramps 1.4. If stepper motors were to be used for the printing, they need to be connected to the Ramps board [18]. These electrical connections are needed to be set once, as an initial step. With using Marlin software, the required changes are completed in a written program by using a computer, which is needed for coupling with the Arduino Mega 2560.

After the electrical connections, the developed head is connected to a 3-axis Computer Numerical Control (CNC) gantry system. Printing materials (continuous carbon fiber and polymer with pellet form) need to be added and syringe cap is seated. The syringe cap have a connection with the Teflon hose by metal connectors, and the hose directly connected to a Nordson EFD air controller. By using Nordson EFD air controller system, a predetermined pressure value can be applied to perform the printing. A heat jacket is also attached to the outer surface of the polymer syringe, for the purpose of heating the pellets. The Arduino controller and a thermistor are used to control the temperature of the nozzle and heat jacket for heating the polymer syringe part.

Moreover, for the printing bed platform, glass is chosen as a bed material to perfectly form adhesion between the deposited materials and the printed bed. After electrical and mechanical setup are prepared, and designed parts are assembled and heated, the printing process can take place. The developed experimental setup can be seen in Figure 22.

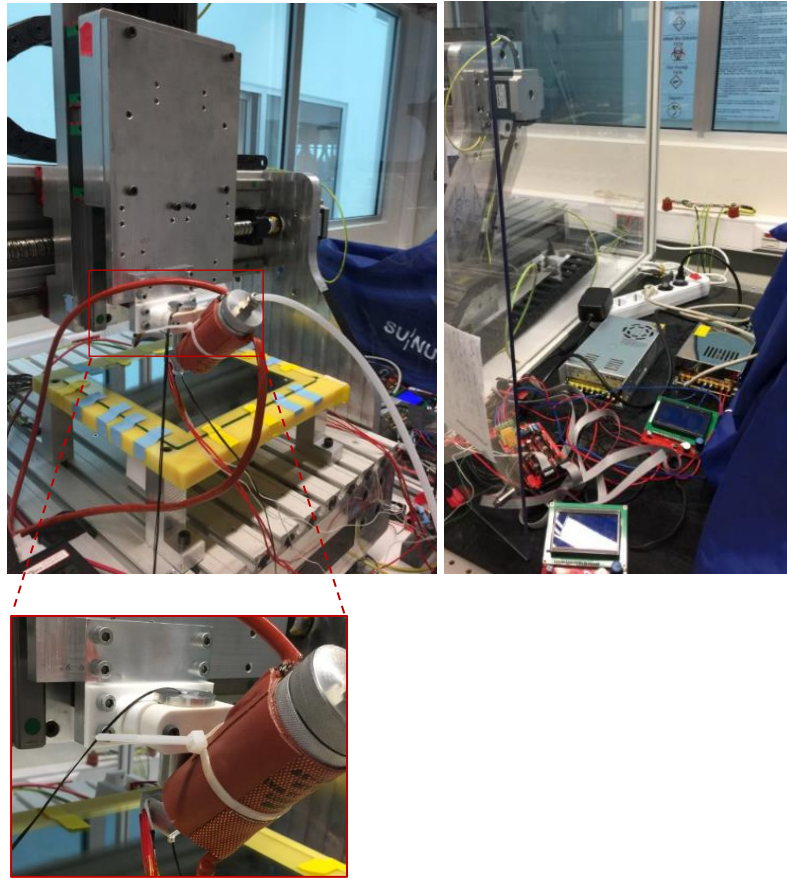


Figure 22: The developed experimental setup.

Before printing process; PLA 4043D pellets and continuous carbon fibers, were supplied separately into the nozzle. Then, the nozzle is heated by using Arduino and heat jacket controllers, for approximately 2 hours. The nozzle and syringe temperatures are controlled individually. First, the syringe is heated and then, the nozzle is gradually heated after that. The reason of heating the syringe primarily is because of the conductivity of aluminum in the design as a thermistor could face problems on monitoring the actual temperature of the nozzle, if insufficient heat is detected. So, to eliminate this problem, initially syringe is heated and after heat jacket's temperature value is increased to the specific point, the nozzle is started to be heated gradually. After the heating process, 3D printing was performed. When the printing is completed, all the used parts (nozzle and syringe) and printing bed need to be cleaned. Mechanical tests were then conducted on 3D printed samples. Tensile and Flexural (3-point bending) tests were performed to observe the effect of using continuous carbon fiber. The general view of the procedure conducted is presented in Figure 23.

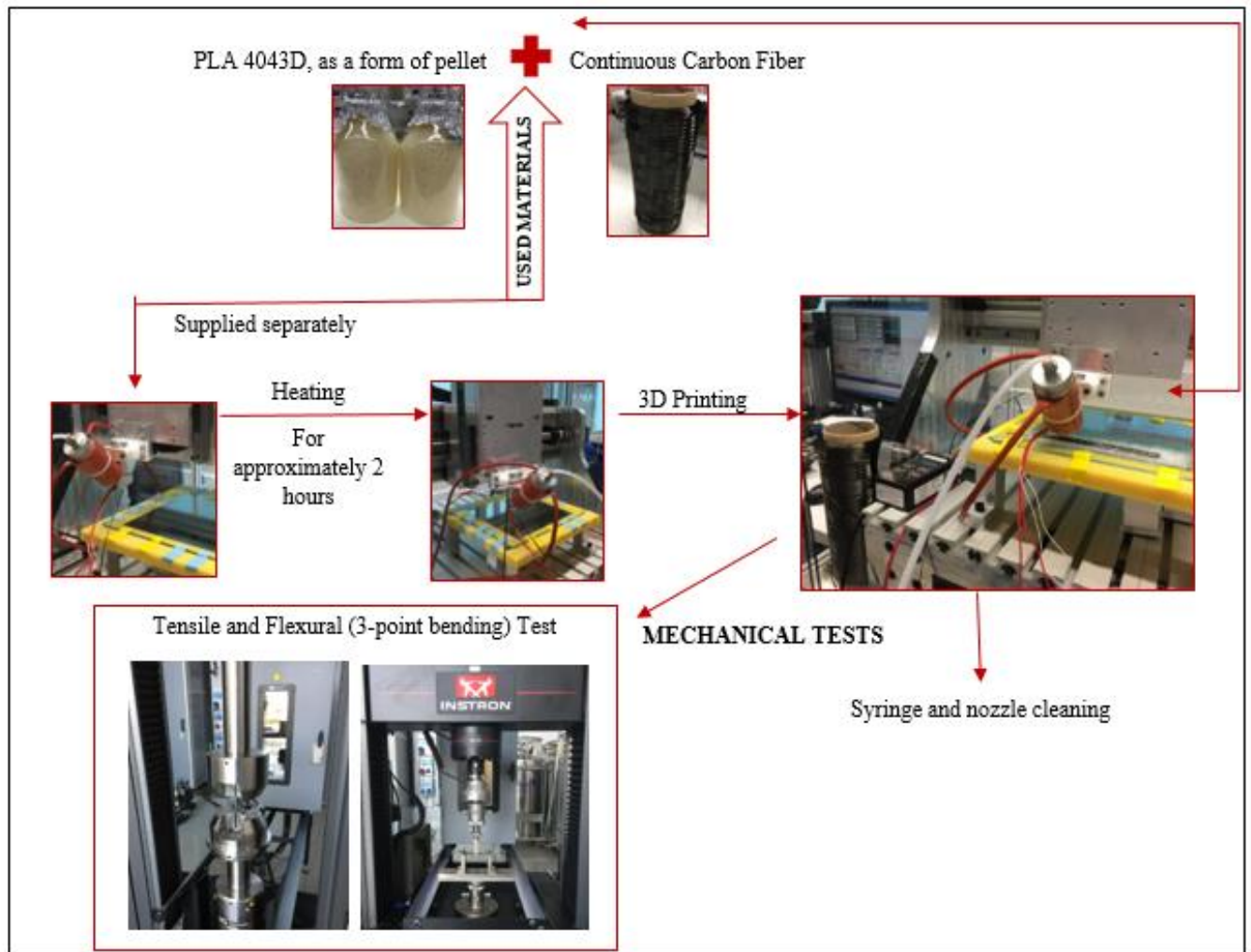


Figure 23: General view of the procedure conducted.

2.4.2 3D Printing preparation and process

2.4.2.1 Simple extrusion

A simple extrusion was performed to test the flow of the materials and to investigate the coaxial view and the concentricity of the supplied materials. In this trial extrusion test, a separate setup was used. This simple extrusion could help to review the general arrangement and the design of the parts.

First, the nozzle was attached to the platform by adjustable clips, and the materials are separately supplied and heated. The heating process is controlled by the Arduino and Heat

jacket controllers similar to the 3D printing setup. Because of the fixed working platform, movements and the x-y-z coordinates cannot be controlled. So, this kind of extrusion can be called as “simple extrusion”, which is mainly used for investigating the separately supplied materials’ concentricity and shapes, especially for the coaxial printing cases. For the simple extrusion, initially, PCL thermoplastic pellets with continuous carbon fiber were used due to their low melting temperatures (around 60-70°C), with continuous carbon fiber. Then, PLA 4043D was also experimented.

By using Nikon Eclipse ME600 optic microscope, images of the coaxially extruded materials were examined and measurements were performed. The obtained images can be seen in Figure 24. The core (dark coloured) material is carbon fiber and outer shell material is thermoplastic polymer.

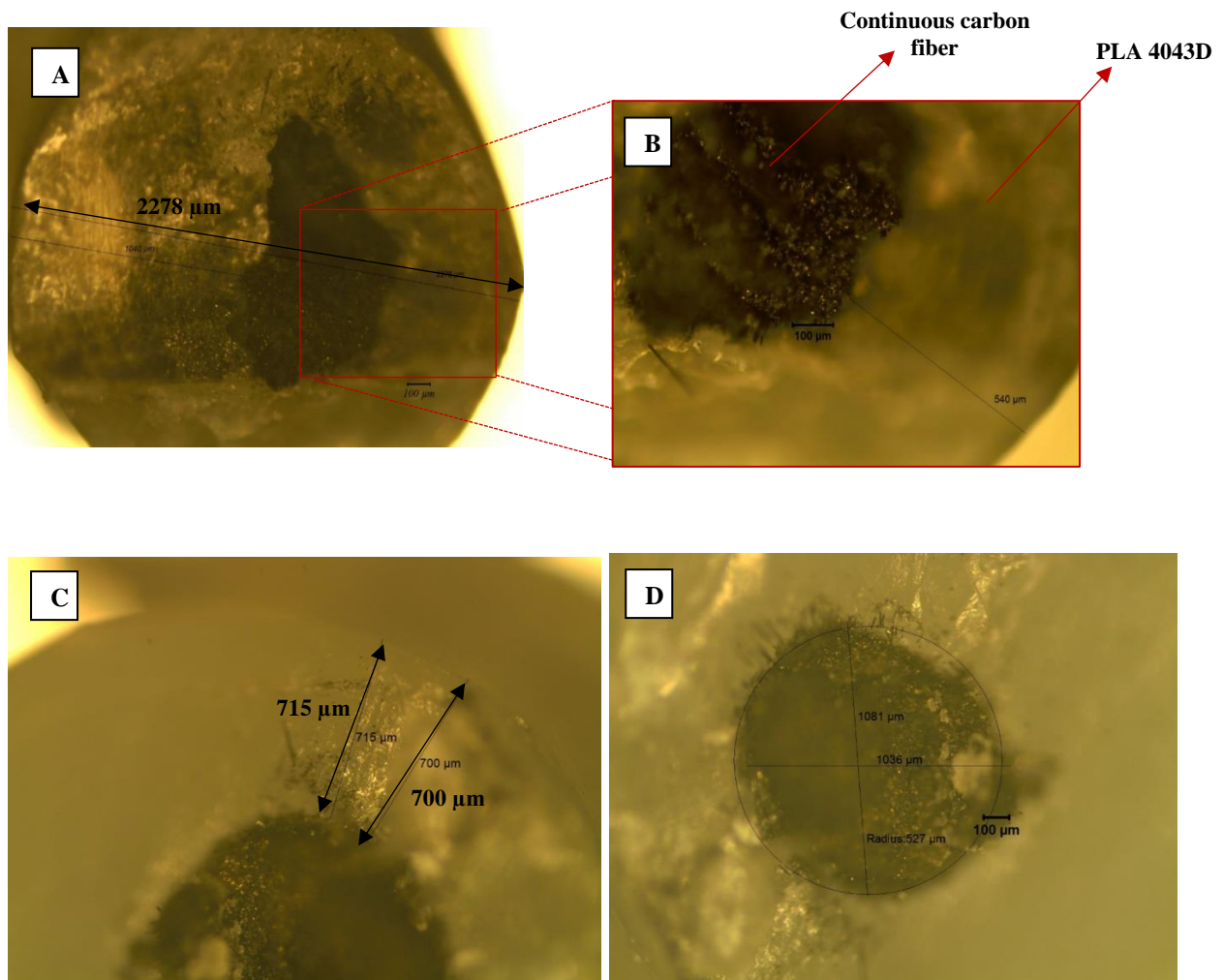


Figure 24: Cross-sectional view of the coaxially extruded materials. (A) and (B) presents coaxially extruded carbon fiber (core) and PLA4043D (shell), with 5X magnification. (C) and (D) presents coaxially extruded carbon fiber (core) and PCL (shell), with 5X magnification.

2.4.2.2 3D Printing

After the simple extrusion, 3D printing was performed for printing the mechanical test samples. The important printing parameters which could directly affect the performance and quality of the printings are: nozzle and syringe temperature, Feed rate (F), Air pressure (P) which is controlled by the Nordson EFD air controller, and the x-y-z coordinates. These parameters need to be optimised and have to be balanced with each other, for better printing results. The nozzle and syringe temperatures are controlled and determined separately. The Feed Rate, Pressure, and x-y-z coordinates are set and controlled by the CNC Code, which is used to create a tool path for the 3D printing. In CNC Code, x-y-z coordinates and feed rate need to be stated. So, in other words, CNC Code is the main controlling building of the motion of the mechanism, and functioning as stating which coordinates the mechanism should move and follow. Printing parameters' units can be seen in the following table (Table 5).

Parameters	Unit
Nozzle temperature	°C
Syringe temperature	°C
Feed rate (F)	mm/min
Pressure (P)	bar
x-y-z coordinates	mm

Table 5: Process parameters and their units.

As an initial step of the 3D printing, levelling of the bed and calibration are required to minimize the possible errors and to perform better printing [18]. After the heating process of separately supplied materials (PLA 4034D and continuous carbon fiber), calibrations were made. The nozzle distance to the printing bed was adjusted and the x-y-z coordinates were set from the program. A sample 3D printing of the continuous carbon fiber and PLA 4043D thermoplastic material can be seen in Figure 25 and 26.

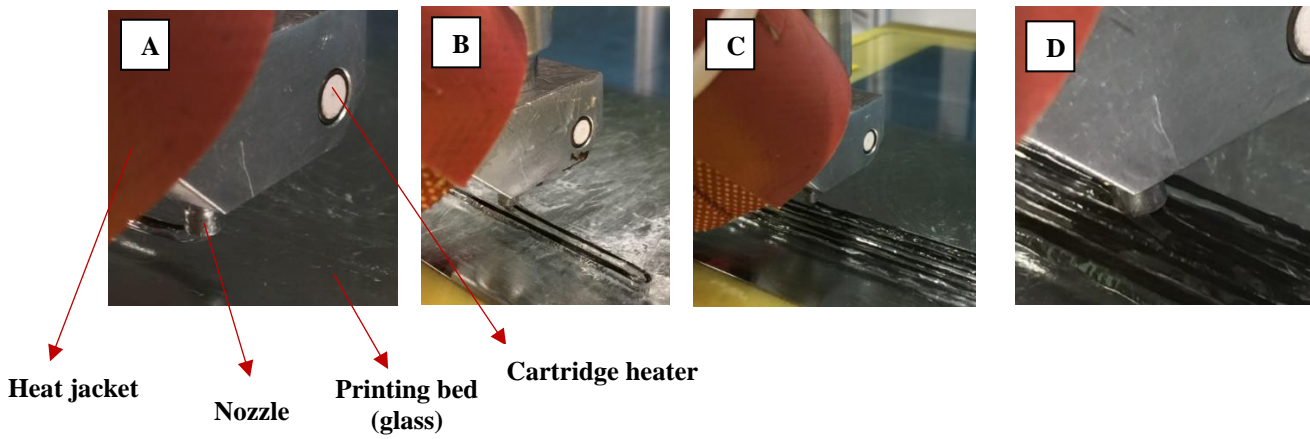


Figure 25: 3D printing process of the continuous carbon fiber and PLA 4043D, starting from the (A) and continues with (B), (C), (D), respectively.

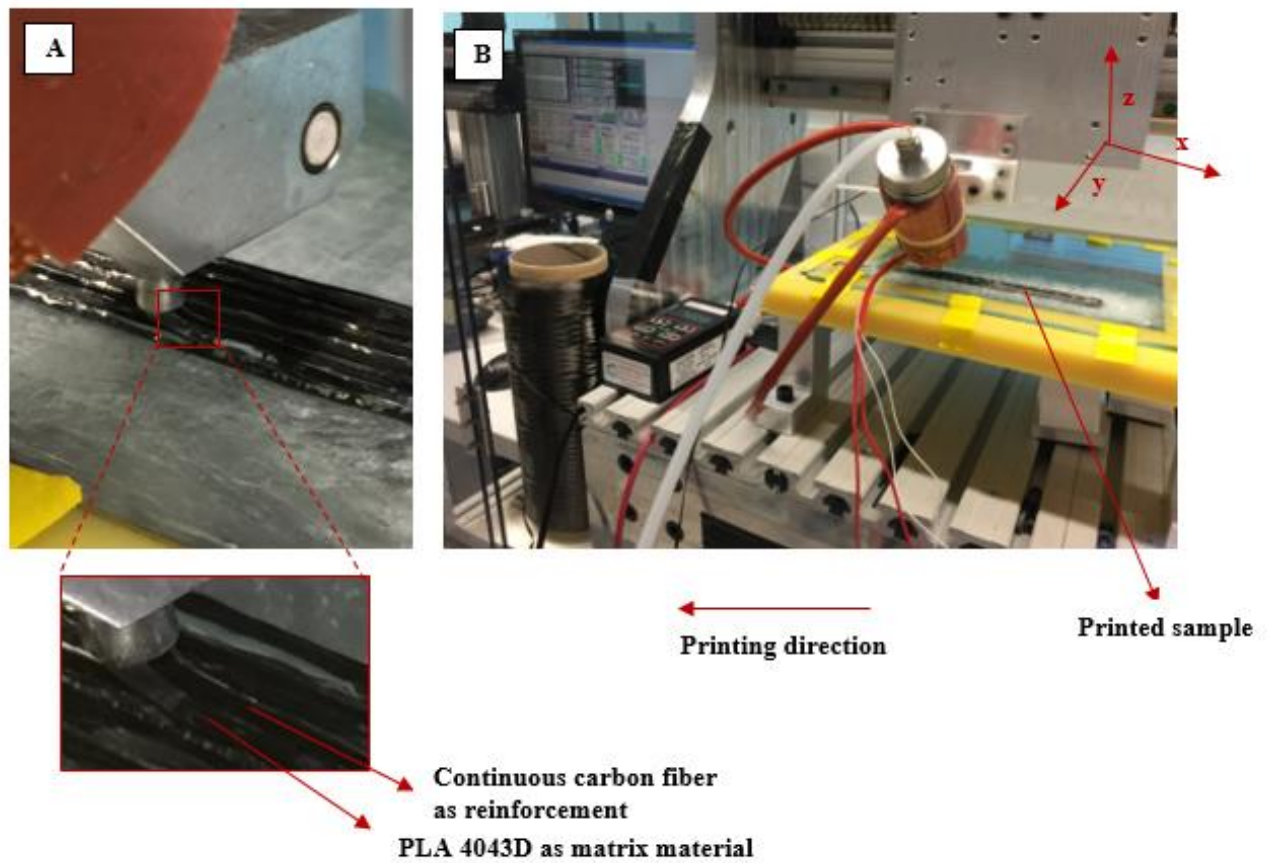


Figure 26: 3D printing with continuous carbon fiber and PLA 4043D. (A) closer view of continuous carbon fiber and PLA 4043D materials, (B) overall view of the 3D printing.

Compared to the simple extrusion, in 3D printing, the traction force is occurred in the opposite direction of the printing. So, it can be stated that, 3D printing can be promoted by the traction force. To improve the traction force, removable adhesives can be applied to the printed bed.

Additionally, pure PLA 3D printing was also performed to compare the mechanical test results with the continuous carbon fiber one. For the pure PLA printing, fiber part needs to be changed and modified part need to be assembled. The 3D printing of pure PLA 4043D thermoplastic material is presented in Figure 27.

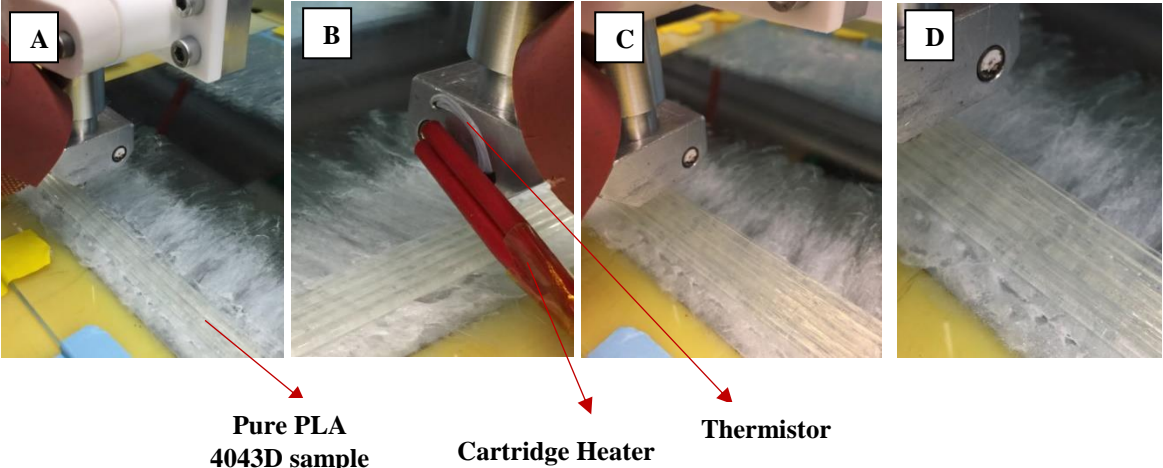


Figure 27: 3D printing of pure PLA 4043D. Starting from (A) and continues with (B), (C) and (D), respectively.

The 3D printed samples' sizes were determined by considering the decided mechanical testing standards (Tensile and Flexural Tests) and their standard test specimen dimensions. Suitable printing paths are formed, and different paths were created for the tensile and flexural test samples separately. A number of stripes of the printed sample, is varied depending on the utilized mechanical test standards. Also, a number of stripes and layer could affect the length of the printing path. Increase on the strip and layer of the sample could directly increase the processing time of the printing. The printing paths follow straight zig-zag patterns as shown in Figure 28 and 29.

For Tensile test specimen; printing path with 6 stripes and 2 layers, was used to perform 3D printing of the determined standard tensile test samples' dimensions. The printing path for the tensile test sample is shown in Figure 28. Also, for the flexural test specimen, printing path includes 5 stripes and 2 layers which can be seen in Figure 29. Arrow indicates the printing direction of the samples. When the 1st layer is completed, the printing of the 2nd layer continued with the reverse printing direction continuously.

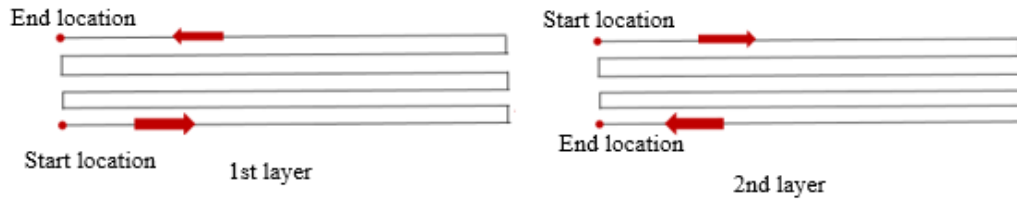


Figure 28: Printing path for the Tensile test specimen.

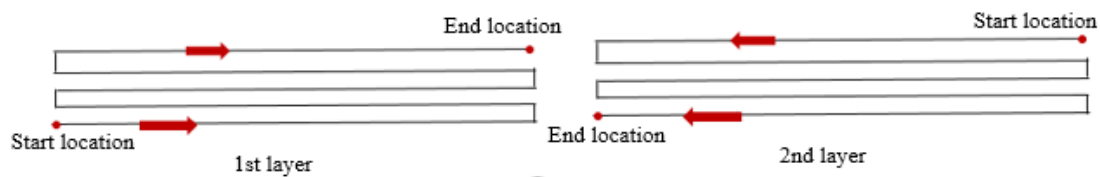


Figure 29: Printing path for the Flexural test specimen.

At the end of the 3D printing, the used nozzle and syringe need to be cleaned for preparing for the next usage. For PCL, acetone and for PLA 4043D, dimethyl sulfoxide (DMSO) were used as a solvent material. Moreover, an oven or a magnetic stirrer was used for heating and mixing the solvent.

2.5 Oxygen plasma as pre-processing technique for carbon fiber

Because the carbon fibers' surfaces could be incompatible with the thermoplastic polymers, weak bonding and adhesion problems could occur between the carbon fiber and the thermoplastic polymer. For increasing the adhesion between the thermoplastic material and fiber, surface treatments can be used for roughening carbon fiber's surface. Hence, compared with the normal surface of the continuous carbon fiber, rougher surface helps to improve the mechanical properties of the printed samples by increasing the bonding and integration with the matrix material. Oxygen plasma is one of the promising pre-processing adhesion improvement technique between the continuous carbon fiber and thermoplastic material. With performing oxygen plasma operations to the continuous carbon fiber, surface treatment of the fiber can be achieved.

Tiwari et al. [55] studied on the carbon fibers' alternative surface treatment operations to increase the adhesion and bonding between the composite materials and implemented as a pre-processing technique. It is stated that carbon fiber's direct usage in the composite, can be resulted in weak interlaminar shear strength, which could directly affect the adhesion between the supplied materials. So, implementation of bonding and adhesion enhancement treatments can be beneficial for performing maximum integration between the continuous carbon fiber and PLA material.

In the oxygen plasma technique, the main goal is to achieve modifications, deteriorations and changes in the surface of the carbon fiber, by using atoms and ions. Oxygen plasma technique is implemented with the objective of improving the adhesion between the continuous carbon fiber and PLA, and able to perform better printings with higher mechanical test results. Two separate fiber pieces from the continuous carbon fiber bobbin, are cut and put inside of the oxygen plasma testing machine, separately. Torr International Inc. machine is used for this experiment, which can be seen in Figure 30.



Figure 30: Torr International Inc. machine, used for oxygen plasma.

Tiwari et al. [55] mentioned in this study that, optimal results can be obtained with the operation duration time of the oxygen plasma technique, is in the range of 1 to 5 minutes. Also, Kolluri et al. [57] stated that operation time of 2 minutes could result in higher deteriorations on the surface of the fiber, which could result in improvements on the mechanical properties. By considering the studies, oxygen plasma experiment is conducted at 100 Watt, and the operation time for one continuous carbon fiber piece is set as 2 minutes, and other continuous carbon fiber piece is set as 3 minutes, to investigate its effects. After the oxygen plasma treatment of the continuous carbon fibers, 3D printing is performed with using the treated fibers. Then, the mechanical tests are conducted to observe the operation's effectiveness.

2.6 Mechanical Tests Methods

The tensile and flexural (3-point bending) tests are performed by UTM (Universal Test Machine) on the 3D printed samples, to investigate continuous carbon fibers' reinforcement effect with the comparison to the pure PLA. Tests are conducted by using Instron testing machines. Before the machine starts to take the real data from the testing sample, the 1N load is exerted to the sample for balancing the system. Also, the extensometer needs to be calibrated, at the beginning of the tensile tests. Stop conditions for the tensile and flexural tests are as follows: for the tensile test, when there exist 40% load loss, the testing machine will stop. For the flexural (3-point bending) test's stop condition, either the test ends when there exist 40% load loss which is similar condition for the tensile test or if there is not that much load loss depending on the utilized ASTM D790 method, the maximum bending percentage that can be reached is defined as 5%. So, the testing will be terminated and the test machine will stop after reaching 5% bending value.

2.6.1 Tensile Test

For the tensile test; the ASTM D638 Standard test method was utilized based on the specified standard. The geometrical presentation of the used ASTM D638 standard test dog-bone sample can be seen in Figure 31.

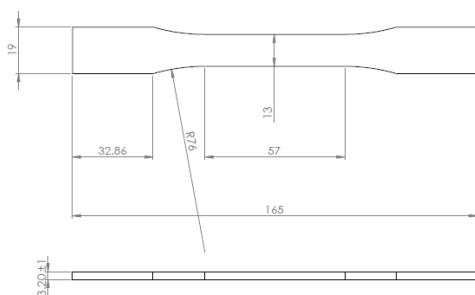


Figure 31: ASTM D638 standard dog-bone sample' dimensions [53].

The tensile test was performed by using the Instron testing machine. 100 kN load cell with an extensometer attachment was used. For testing, gauge length was defined as 57 mm in the BlueHill program, which was directly taken from the applied ASTM D638 standards (Figure 32).

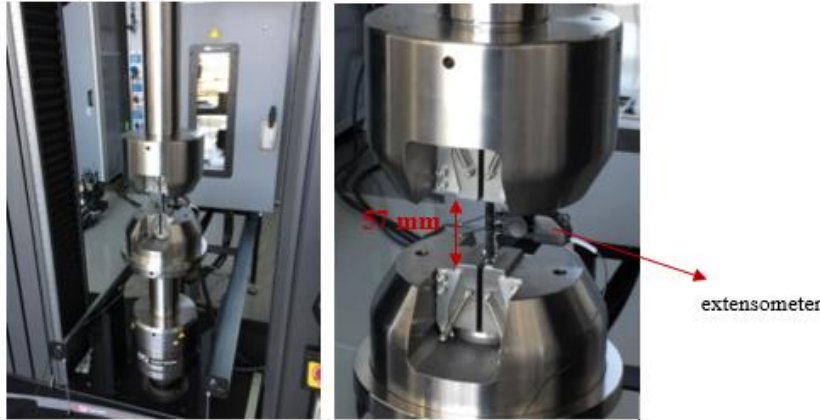


Figure 32: Instron tensile testing machine with the testing sample.

The tensile strength can be calculated by using the following equation shown in Table 6.

Tensile Strength Eqn.	$\sigma = \frac{F}{bt}$	F= stretching force (N) b = width of specimen (mm) t = thickness of sample (mm)
-----------------------	-------------------------	---

Table 6: Tensile strength equation [11].

The tensile test samples were printed in a rectangular shape instead of the dog-bone, by considering on the ASTM D638 standard test specimens' sizes, because with using continuous carbon fiber, the dog-bone shaped printing could result in difficulties on the printing path's continuity and directly cause void formation. The length of the sample is taken as 165 mm, width is taken as around 13 mm and thickness is around 3,20 mm, which are specified in the standard sizes. Because of having rectangularly shaped samples, tabbing needs to be performed before the tensile tests. Tabbing is used to make sure the fracture locations of the sample happens in the middle section. By tabbing, the rectangular shaped printed samples behaved as dog-bone samples so to control and hold the fracture site in the middle section. As the initial stage, 0,5 mm rectangular aluminium tabs were taken and their edges were ground. Then, tab's surface which will be in the contact with the sample, was determined and ground by sandpaper. To remove the possible dust that is formed during the grinding process, the ultrasonic cleaner was used and tabs were put inside of the ultrasonic bath for 180 seconds. To bind the tab with the samples, Huntsman Araldite 2011-A/B was used [54]. After the application of Araldite on the samples, tabs were fixed on the sides, and curing was required for complete drying of the

adhesive. Due to the PLA low melting temperature, curing at the room temperature (20°C) is preferred and curing time was extended to 1 day. After the application of Araldite 2011 and curing at room temperature, the tabbed samples were used in the tensile test. The prepared reinforced carbon fiber and pure PLA samples with tabs are shown in Figure 33.

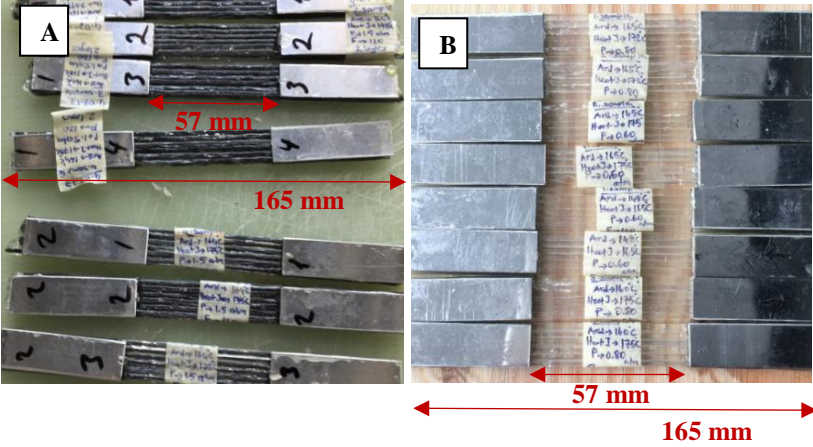


Figure 33: Prepared samples with 0,5 mm aluminium tab. (A) Continuous carbon fiber reinforced PLA samples, (B) Pure PLA samples.

2.6.2 Flexural Test

For the flexural (3-point bending) test; the ASTM D790 Standard test method was utilized and the tests were performed based on the specified standard.

The flexural test was performed by using the Instron flexural testing machine, with an attachment of 3-point bending head. A 5 kN load cell capacity was used in the test machine, which resulted in longer testing time compared to using 100 kN load cell. The rate of displacement is defined as 2 mm/min and span length is determined as 80 mm (Figure 34).

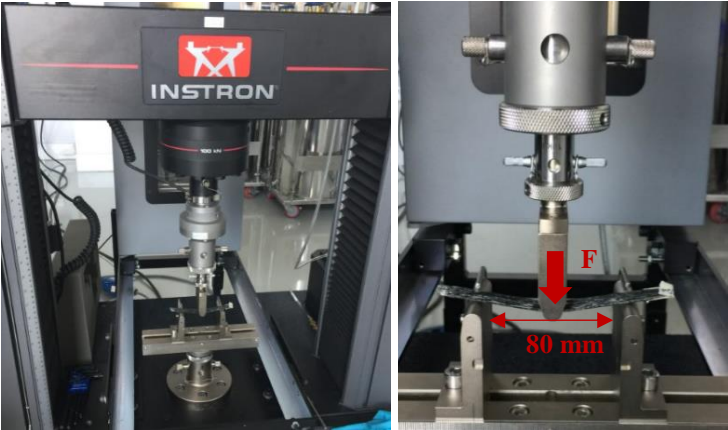


Figure 34: Flexural testing machine, with testing sample.

The flexural stress, strain and modulus can be calculated by using the following equations shown in the Table 7.

Flexural Stress Eqn.	$\sigma = \frac{3PL}{2bt^2}$	σ = Flexural Stress (MPa) P = Load (N) L =Support span (mm) b = width of specimen (mm) t = thickness of sample (mm)
Flexural Strain Eqn.	$\varepsilon = \frac{6dt}{L^2}$	ε = flexural strain (mm/mm) d = deflection (mm)
Flexural Modulus Eqn.	$E = \frac{FL^3}{4dbt^3}$	E= flexural modulus F= force on the center of the beam

Table 7: Flexural stress, strain and modulus calculations [41,45].

2.7 Tensile following microwave oven application as post-processing

The microwave oven was utilized as a post-processing technique to investigate its effect for improving the bonding between the stripes and layers of the printed samples. Stronger and integrated bonding properties could directly contribute the mechanical properties of the samples. As stated previously, a thermal bonding can be improved by using a microwave oven [51]. With the thermal bonding process, the chemical bonding of the sample could be enhanced by the applied heat and adhesion between the layers. Microwave oven effect is analyzed for both the printed samples of carbon fiber reinforced and the pure PLA. To investigate the effect of microwave usage in the most accurate condition, one long specimen with the length of 180 mm, was printed by a newly generated CNC Code. After the printing process of the sample, the printed long specimen is separated into two from the middle point. By doing this, possible parameter differences between the parts could be eliminated and the resultant two samples have completely the same features. Hence, microwave effect could be directly observed. After the separation of the long sample, one of the separated piece, which has the length of 90 mm, was placed into the microwave oven. For carbon fiber reinforced and pure PLA printing, microwave oven's power (W) and processing time values (in seconds), are changed to find optimum values. At first trial, the power was set as 800W and the heating process duration as 60 seconds, for the both, carbon fiber reinforced and pure PLA printed samples. There was no problem observed with the pure PLA case for the initial set values. However, for continuous carbon fiber reinforced PLA case, due to the conductivity of carbon, PLA started to melt and some samples

started to change their shapes at the end of the heating process. So, it was determined that lower values are needed (for power used and the operation duration), especially for the fiber reinforced samples, to perform the controllable heating process.

After the performed initial test with carbon fiber reinforced PLA, microwave oven test was repeated with the lower values; in 300 Watt for 15 seconds. The heating process is completed without any problem.

3. RESULTS & DISCUSSIONS

3.1 Printed parts qualitative characterisation

Pure PLA and continuous carbon fiber reinforced PLA printings were performed to compare their mechanical results. The different nozzle and syringe temperatures, Pressure (P) and Feed Rate (F) values were tested and their effects on the mechanical tests were studied. The ranges of these tested parameters are; nozzle (controlled by Arduino) temperature in the range of 145-170°C, syringe (controlled by heat jacket controller) temperature in the range of 165-178°C, pressure values in the range of 0.5-1.80 bar, and finally, feed rate values in the range of 110-150 mm/min. The first layer's thickness (z coordinate value) is 1.8 mm and the second layer has the z coordinate value of 3 mm. During the printing, the nozzle temperature values were kept lower compared to the syringe temperature. Some of the printed continuous carbon fiber reinforced PLA and pure PLA printing samples can be seen in Figure 35 and 36, respectively.

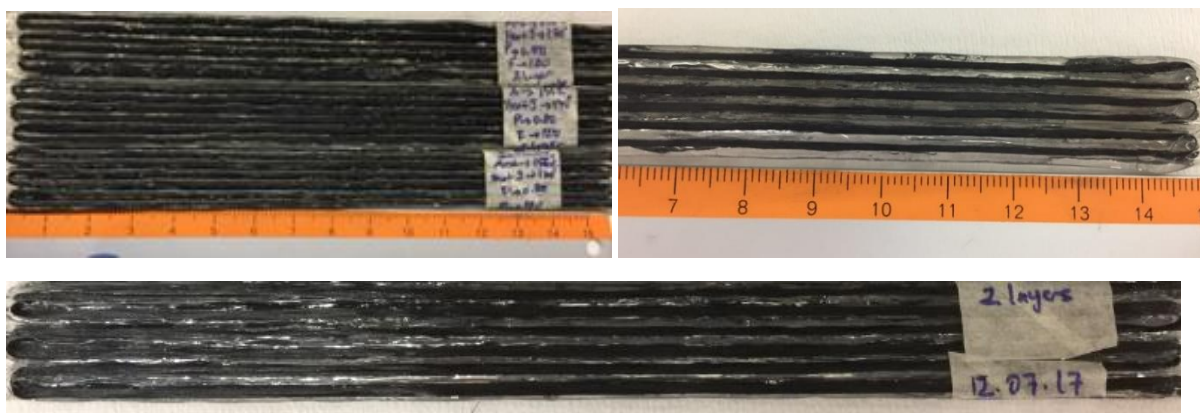


Figure 35: 3D printed continuous carbon fiber reinforced PLA samples.

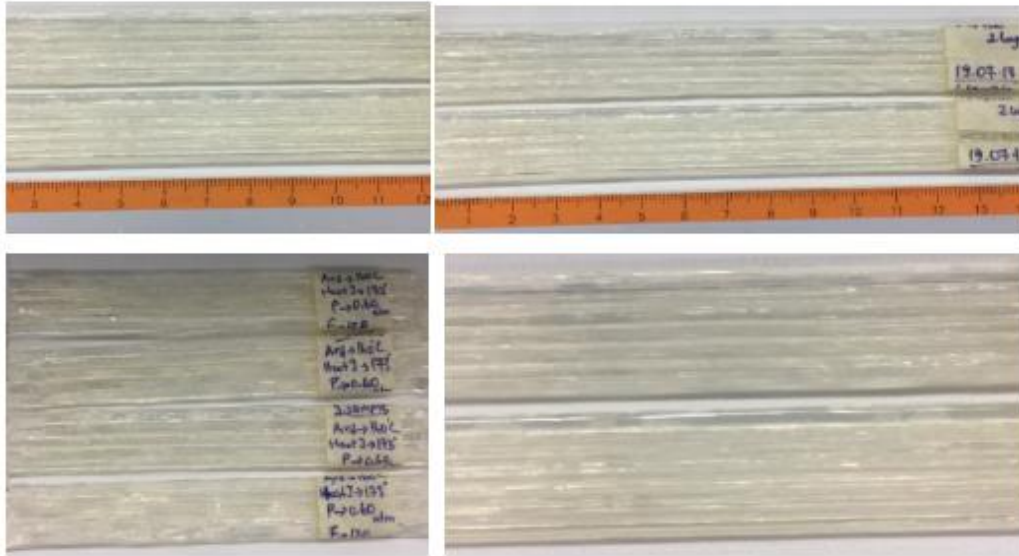


Figure 36: 3D printed pure PLA samples.

Totally, 124 samples were printed and tested. 63 samples were tested by using the tensile test and 61 samples were tested with using the flexural test. In some of the printings, defects and problems are observed. Therefore, defective printed samples were excluded from the mechanical tests.

As mentioned in the introduction chapter, continuous carbon fiber usage can cause some problems, which can directly affect the samples' printing quality, surface roughness, and mechanical properties. One of the main problems is; weak adhesion between the deposited materials and between the deposited layers and stripes. Adhesion is one of the most critical element which affects mechanical properties of the printed composite parts. Adhesion problems between the materials can easily exacerbate the defects and led to lower mechanical properties. Also, low adhesion between the deposited layers and stripes can increase the void formation and weaken the mechanical properties of the samples.

During 3D printing of the continuous carbon fiber reinforced PLA and pure PLA, a weaker adhesion problem was observed, especially in the continuous carbon fiber reinforcement case. The surface of continuous carbon fibers' surface was not very compatible with PLA and this resulted in imperfect adhesion and weak bonding between the layers. For increasing the adhesion between the carbon fiber and polymer, pre-processing techniques can be applied for changing and roughening of the surface of fibers. Thus, chemical bonding between the fiber and PLA can become stronger and lead greater mechanical properties. Some of the applicable

pre-processing adhesion improvement techniques can be; plasma, gamma, and oxidation treatments. [55]. By performing these techniques, more integration between the fiber and thermoplastic polymer can be achieved and polymer can successfully diffuse into the fiber. Additionally, due to the carbon fibers' tendency of void creation between the layers [36,37], lower mechanical results can be obtained. The experimented samples with the problem of weak adhesion and bonding, is shown in Figure 37.

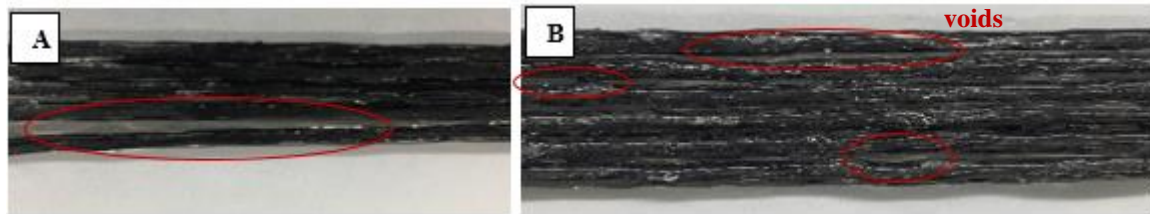


Figure 37: Printed samples with the problem of adhesion. (A) adhesion problem between the stripes, (B) weak bonding and void problems.

Moreover, printed samples need to have certain adhesion with the printing bed in order to create sufficient traction force. Otherwise, printed stripes cannot be attached to the surface and sliding can happen during the printing process, which can result in poor printing. To encourage the adhesion between the printing bed and the material, adhesive can be used.

3.1.1 Scanning electron microscopy (SEM) imaging of printed parts

As stated before, the poor adhesion between the deposited materials is one of the key reasons for not achieving perfect and desired mechanical properties. Adhesion problems have a direct effect on the mechanical performance of the printed parts. Especially in composite printing, adhesion quality has a significant impact to improve the mechanical strength of the parts. Using continuous carbon fiber in 3D printing is difficult because the surface of carbon fibers is not very compatible with thermoplastic polymers. Hence, as a solution, it is suggested by researchers that pre-processing techniques can be applied to increase the chemical bonding between the fiber and matrix, which can improve the mechanical properties of the printed samples [55]. The diffusion and adhesion problems were observed in this study. Cross-sectional

views of the printed samples were analyzed to investigate these problem closely and to show the bonding between the layers and materials.

For the preparation process of the cross-sectional specimens for the microscope visualization, cold mounting is used. For cold mounting applications, EpoFix resin and hardener, and FixiForm as a mold, are used. EpoFix resin and hardener need to be mixed in the separate pot, according to the stated mixture rate which is; for EpoFix resin, 25 parts by weight of the resin pouring and for hardener, 3 parts by weight of the hardener pouring. The printed parts were fixed on the aluminum tab, for making samples stable inside the epoxy-filled mold. Then, the prepared mixture was poured into the mold and cured at the room temperature, which took approximately 1 day. Then, the dried epoxy-filled parts were ground using sand papers. Starting with the coarsest sand paper of 320, sand papers of 500, 1000, 2400 and 4000 were used respectively, for 4 minutes operation time for each sample. After that, epoxy-filled samples were cleaned by ultrasonic cleaner and they were examined under the microscope.

By using scanning electron microscope (SEM), cross-sectional images of 2-layered carbon fiber reinforced PLA, and pure PLA were examined and shown in Figure 38. Since the epoxy resin and PLA had similar light color, it was difficult to directly distinguish them. By considering the boundaries, the materials can be distinguished easily. Black colored dots represent continuous carbon fibers. Figure 38 (A) shows zoomed cross-sectional part of the continuous carbon fiber reinforced PLA sample. Some fiber distribution can be observed but, total diffusion cannot be seen. Also, some voids can be observed between the printed layers. Figure 38 (B) presents pure PLA samples and as can be easily seen from the image, there is better integration between the layers with lesser voids, compared with the Figure 38 (A) and (C). Figure 38 (C) also shows the carbon fiber reinforced PLA sample and the diffusion problem can be observed as in Figure 38 (A). Thus, it can be stated, there exist diffusion and adhesion problem in carbon fiber reinforced case, because of the incompatibility between for the surface of carbon fibers and the thermoplastic polymers (such as PLA).

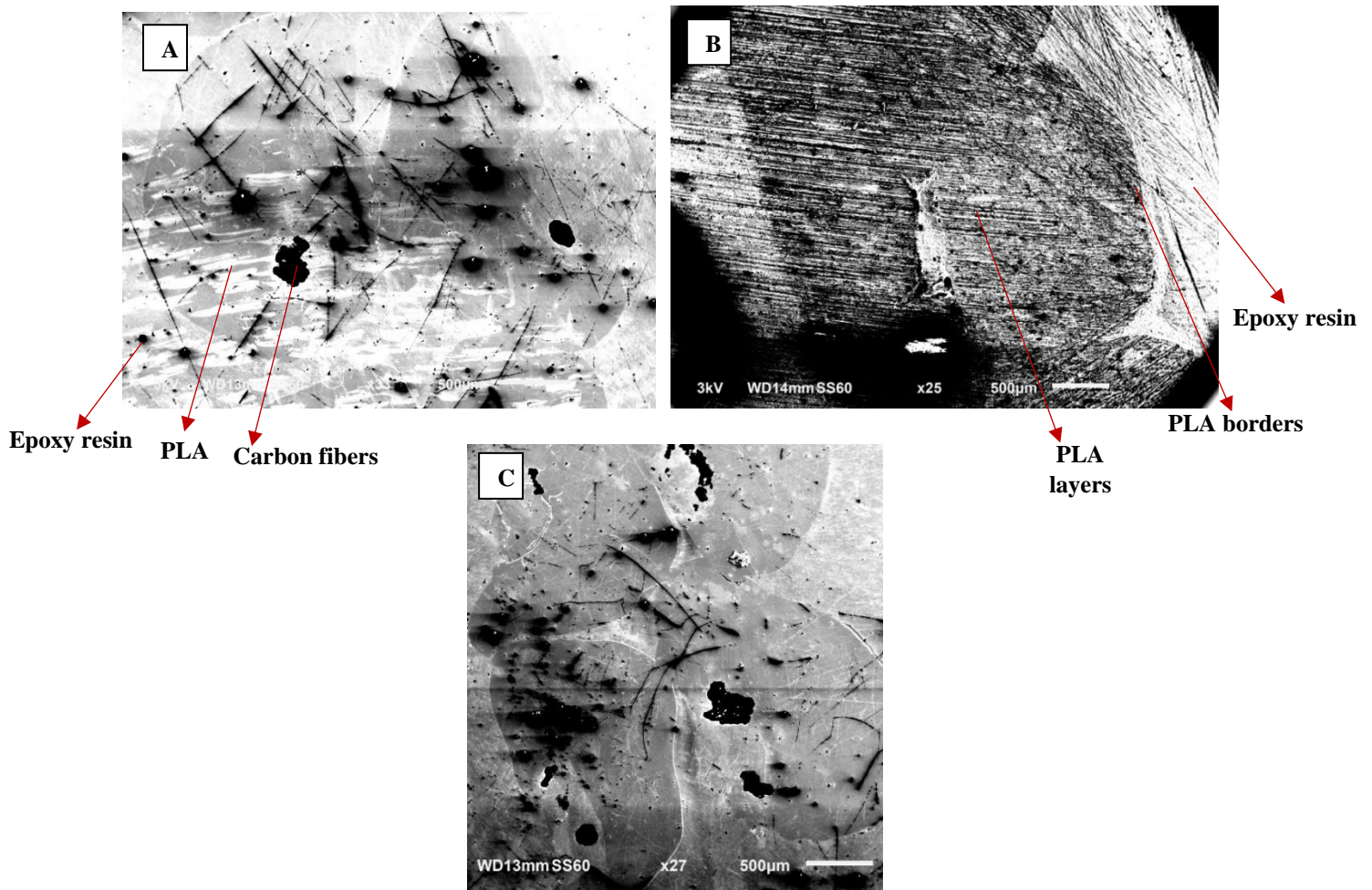


Figure 38: SEM cross-sectional view of 2-layered carbon fiber reinforced and pure PLA. (A) carbon fiber reinforced PLA sample, (B) pure PLA sample, (C) carbon fiber reinforced PLA sample.

The volume fraction for the carbon fiber volume (V_f) is calculated by using Equation (1) [11]. In Equation (1), A_f symbolizes the used carbon fiber's cross section area and A symbolizes the total area of the polymer and carbon fiber. Also, the assumption is made that the carbon fiber and the thermoplastic polymer materials are deposited in the perfect circular shape. Based on the materials used, the carbon fibers and the total fiber and polymer diameters are taken as 1,5 mm and 2,5 mm, respectively. By using the Equation 1, the carbon fiber volume fraction is calculated to be 36%.

$$V_f = \frac{A_f}{A} \times 100\% \quad (1) [11]$$

3.1.2 Scanning electron microscopy (SEM) imaging of oxygen plasma technique

By using scanning electron microscope (SEM), normal (untreated), 2 minutes treated and 3 minutes treated continuous carbon fibers were examined to visualize changes or deteriorations in the surface of the fibers. The obtained SEM images are presented in Figure 39. As can be seen in Figure 39 (C) and (D), the treated fibers show rougher surfaces compared to the untreated fibers. Hence, oxygen plasma method is applicable method for achieving changes and deteriorations on the surface, which can results in improvements of the mechanical properties.

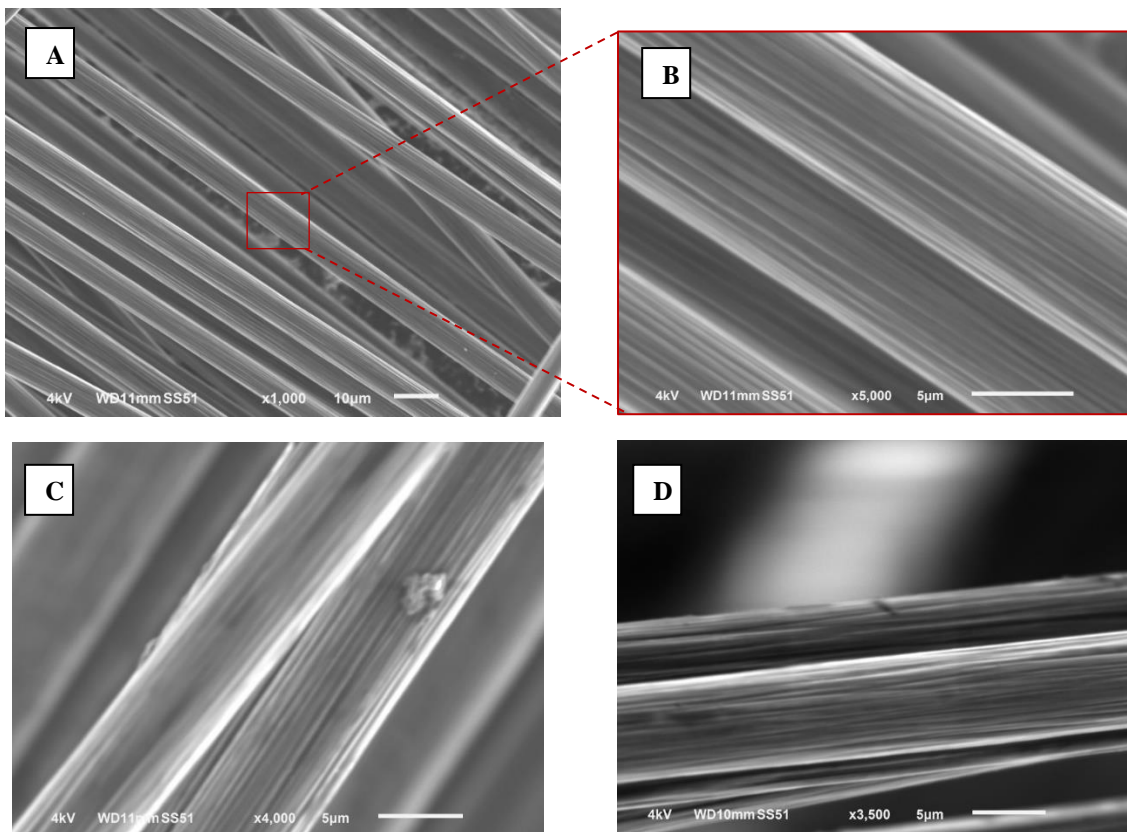


Figure 39: SEM image of the Normal (untreated), 2 minutes treated and 3 minutes treated continuous carbon fiber. (A) untreated fiber in general perspective, (B) untreated carbon fiber, (C) 2 minutes treated carbon fiber, and (D) 3 minutes treated carbon fiber.

Also, it is important to note that, to obtain the greatest improvements and fully benefit from the oxygen plasma treatments of the fiber, they need to be printed immediately. Otherwise, the desired improvements may not be observed. If not printed immediately, the treated fibers need to be placed in a desiccator under the vacuum, to preserve them from the direct contact with air. Otherwise, the expected results and improvements may not be achieved.

3.2 Mechanical Tests

3.2.1 Tensile test

Tensile test were performed separately on the 3D printed pure PLA and continuous carbon fiber reinforced PLA samples. The analysis was conducted between the pure and carbon fiber reinforced PLA material, and at the same time, the samples within the same property were also compared to determine the best printing parameters.

The pure and continuous carbon fiber reinforced PLA's tensile strength values, were examined and plotted in Figure 40. The printed samples mean values were taken and according to the tensile strength comparison based on the means, by reinforcing PLA with continuous carbon fiber an approximately %42 improvement was obtained. Resulting in less than expected improvements is mainly due to the adhesion and diffusion problems, which are the main problems with carbon fiber usage and these problems are also visualized by SEM images. Based on obtained results, in the comparison of carbon fiber and pure polymer, it can be stated that carbon fiber reinforcement can improve the mechanical properties of the pure thermoplastic polymer. However, due to the weak bonding, adhesion and diffusion problems, much higher improvement values cannot be obtained.

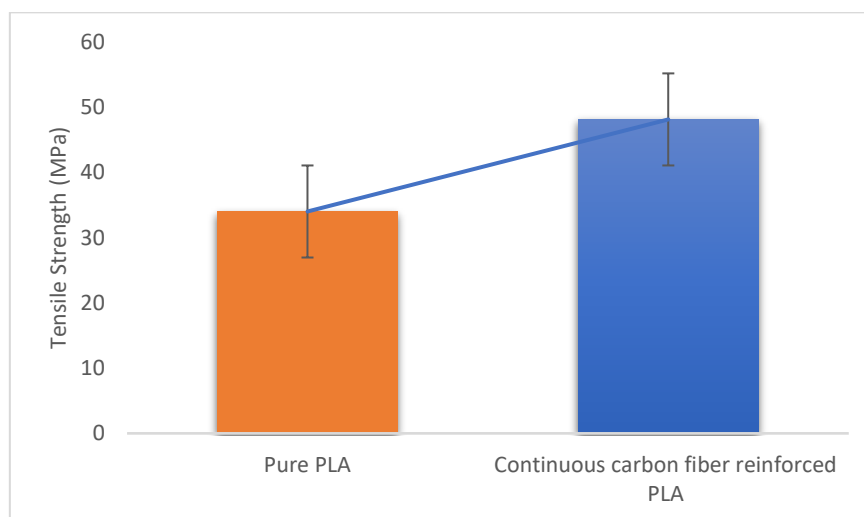


Figure 40: Tensile strength comparison of pure and continuous carbon fiber reinforced PLA' mean values.

To investigate the effects of the printing parameters on the tensile strength of the samples, the tensile tested continuous carbon fiber reinforced sample' mean values were examined for various printing parameters. The obtained results can be seen in Figure 41. According to the graph, the best tensile strength result was obtained with the parameters of; Nozzle temperature of 163°C, syringe temperature of 170°C, Pressure of 1.8 bar and Feed rate of 120 mm/min, (shown as green color). The second-best result was obtained with the parameters of; Nozzle temperature of 166°C, syringe temperature of 173°C, Pressure of 1.6 bar and Feed rate of 150 mm/min, and the third-best result was with the Nozzle temperature of 164°C, syringe temperature of 175°C, Pressure of 1.5 bar and Feed rate of 120 mm/min parameters.

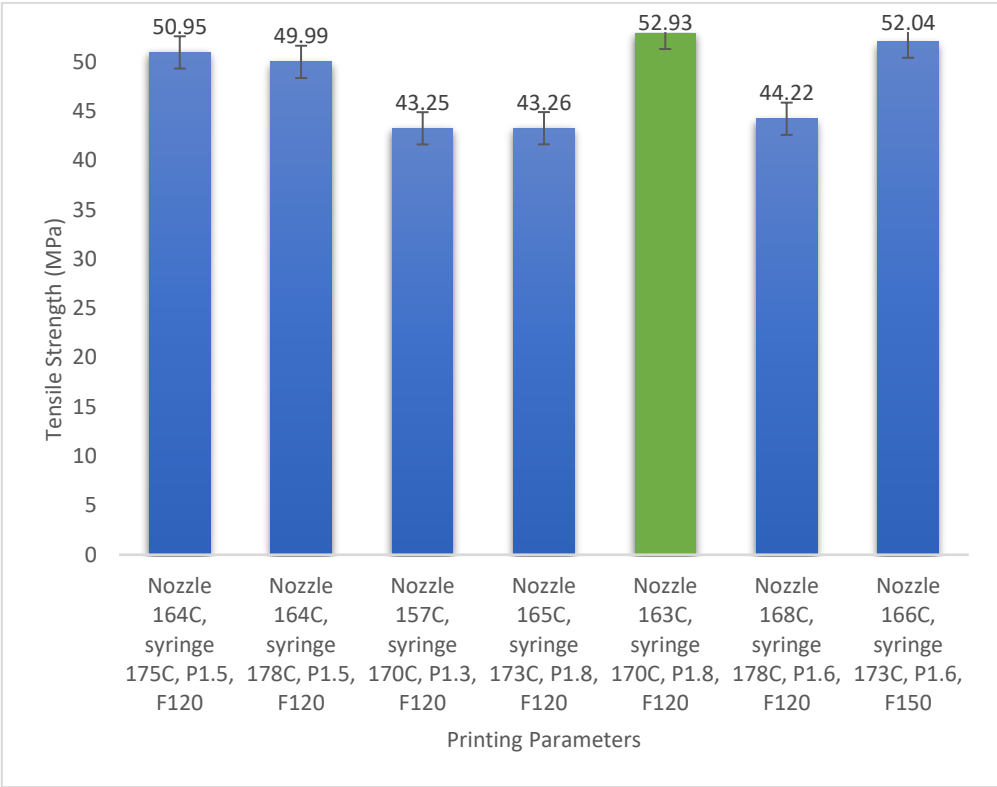


Figure 41: Tensile strength comparison with different printing parameters of continuous carbon fiber reinforced PLA samples.

Moreover, pure PLA samples' printing parameters were also compared. The obtained results can be seen in Figure 42. The best tensile strength result was obtained with the parameters of; Nozzle temperature of 165°C, syringe temperature of 172°C, Pressure of 0,8 bar and Feed rate of 120 mm/min.

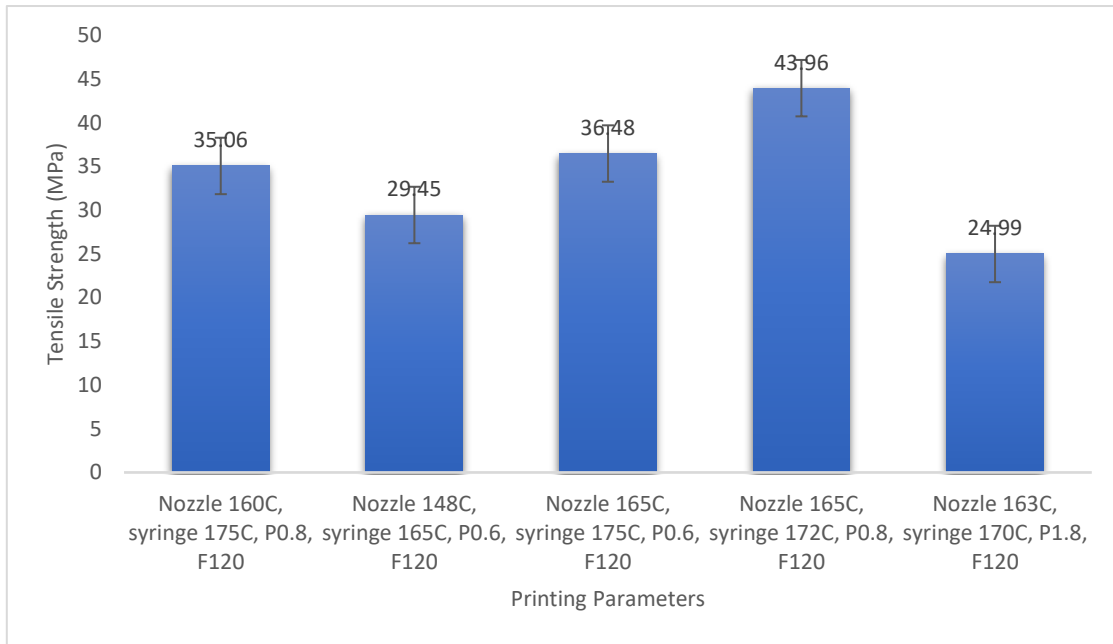


Figure 42: Tensile strength comparison with different printing parameters of pure PLA samples.

Importantly, to investigate the exact improvement obtained by using continuous carbon fiber reinforced PLA, and to compare the results with the pure PLA, the printing parameters were kept same. The optimum printing parameters are taken as; Nozzle temperature of 163°C, syringe temperature of 170°C, Pressure of 1.8 bar and Feed rate of 120 mm/min for both, carbon fiber reinforced and pure cases, which was the best printing condition for continuous carbon fiber reinforced PLA samples, as shown previously in Figure 41. The improvement and the values of the comparison of pure and carbon fiber reinforced PLA with the same printing parameter, can be seen in Figure 43.

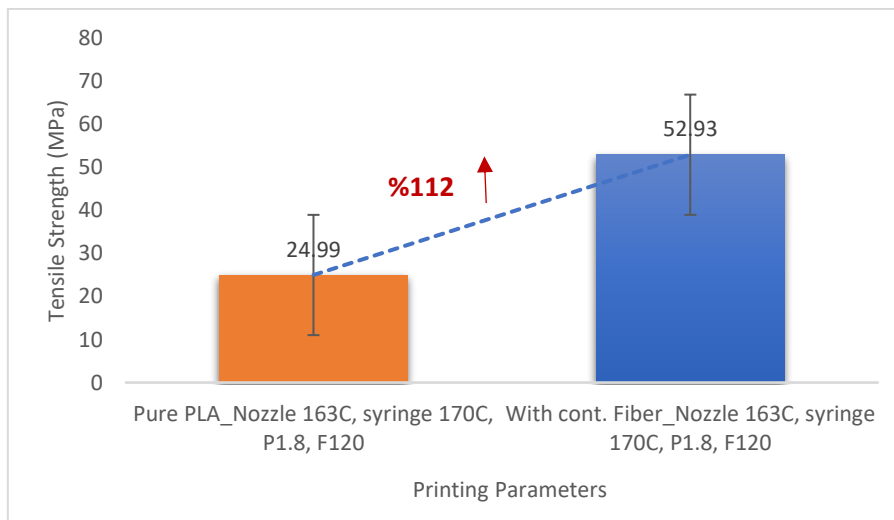


Figure 43: Tensile strength comparison of pure (left) and continuous carbon fiber reinforced PLA (right), with the parameters of; Nozzle 163°C, syringe 170°C, Pressure of 1.8 bar and Feed rate of 120 mm/min.

Depending on the obtained results, %112 improvement in the tensile strength was observed with the continuous carbon fiber reinforced PLA, compared to the pure PLA samples. With using the same printing parameters, the exact effect of the continuous carbon fiber effect can be seen. Therefore, it can be stated that continuous carbon fiber involvement as a reinforcement, enhanced the tensile strength by %112, in the comparison of pure PLA ones.

Also, by using the same printing parameters which are; nozzle temperature of 163°C, syringe temperature of 170°C, Pressure of 1.8 bar and Feed rate of 120 mm/min for both, the carbon fiber reinforced and the pure cases, the load vs. extension graph can be seen in Figure 44. According to the graph, higher load value can be obtained by using continuous carbon fiber as a reinforcement. Moreover, it can be observed that pure PLA was broken directly but, the continuous carbon fiber reinforced PLA can bear higher loads even there exist some cracks.

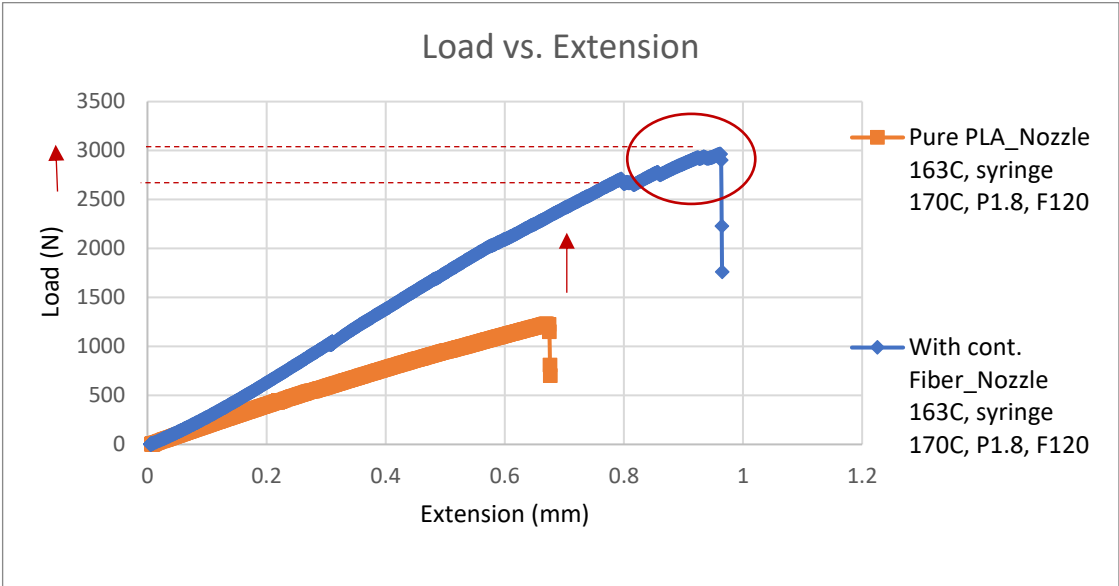


Figure 44: Load vs. Extension comparison of pure and continuous carbon fiber reinforced PLA, with the parameters of; Nozzle 163°C, syringe 170°C, Pressure of 1.8 bar and Feed rate of 120 mm/min.

3.2.2 Flexural test

Flexural (3-point bending) test were performed separately on the 3D printed pure PLA and continuous carbon fiber reinforced PLA samples, and the data is obtained.

The flexural stress (MPa) and strain (mm/mm) values, with different printing parameters for the pure PLA samples, can be seen in Figure 45.

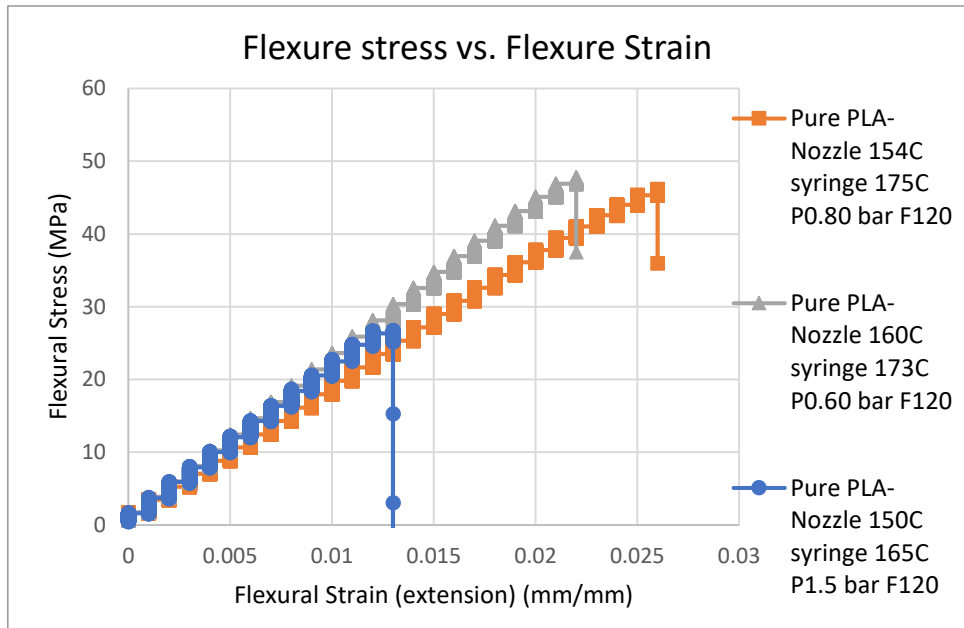


Figure 45: Flexural stress and strain comparison of pure PLA samples.

The continuous carbon fiber reinforced PLA samples' flexural stress (MPa) and strain (mm/mm) values, are presented in Figure 46.

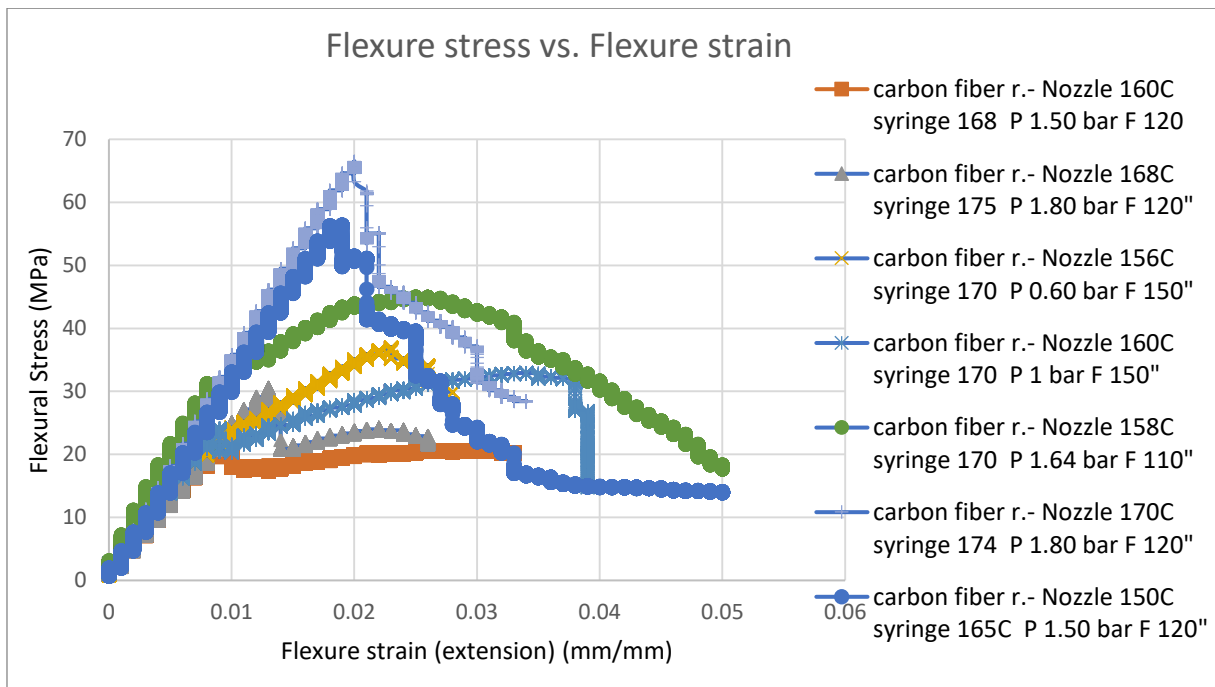


Figure 46: Flexural stress and strain comparison of continuous carbon fiber reinforced PLA samples, with various printing parameters.

The continuous carbon fiber reinforced PLA samples with various printing parameters were experimented. Based on the results (Figure 46), the best flexural stress is obtained with the parameters of; Nozzle temperature of 170°C, syringe temperature of 174°C, Pressure of 1.8 bar and Feed rate of 120 mm/min. Also, the best flexural strain value is obtained with the parameters of; Nozzle temperature of 150°C, syringe temperature of 165°C, Pressure of 1.5 bar and Feed rate of 120 mm/min.

For pure and continuous carbon fiber reinforced PLA flexural stress and strain comparison; in pure PLA cases, as the biggest difference, the linear graph was observed. This is because of the usage of the pure material. That is to say, due to the lack of the reinforcement material, the pure PLA samples directly went to the load and broken immediately. On the other hand, in the continuous carbon fiber reinforced PLA cases, because of the continuous carbon fiber usage as a reinforcement, immediate breaking situations were not observed. The maximum stress obtained from pure PLA samples is approximately 47 MPa. This value is 66 MPa, for the continuous carbon fiber reinforcement PLA samples.

Moreover, in continuous carbon fiber reinforced PLA samples, the flexural strain values are greater than pure PLA ones. In two tested parameters, which are; Nozzle temperature of 150°C, syringe temperature of 165°C, P 1.5 bar and F 120 mm/min (represented in dark blue), and Nozzle temperature of 158°C, syringe temperature of 170°C, P 1.64 bar and F 110 mm/min (represented in green), extension is reached to 0.05 mm/mm which is %5. This strain value is approximately 0.025 mm/mm, which is %2.5, for pure PLA sample. This situation can be explained as; pure PLA directly broke, when some layers or stripes are deformed and cracks are formed. Small cracks can propagate quickly because of the PLA thermoplastic polymer structure and lack of the reinforcement. In the continuous carbon fiber reinforced PLA sample, although the thermoplastic polymer was deformed, carbon fibers can still withstand the loads, which directly increase the durability of the samples.

In the flexural test, the improvement obtained by using continuous carbon fiber reinforced PLA can be analysed by using the same printing parameters and directly comparing the flexural strength results of the carbon fiber used samples with the pure PLA ones. The printing parameters are selected as; Nozzle temperature of 150°C, syringe temperature of 165°C, P 1.5 bar and F 120 mm/min for both, carbon fiber reinforced and pure PLA cases. This printing parameters gave the best flexural test results for the continuous carbon fiber reinforced PLA samples, which can be seen in the flexure stress and strain graph, in Figure 46. The improvement

and the values of the pure and the carbon fiber reinforced PLA samples with the same printing parameter, can be seen in Figure 47.

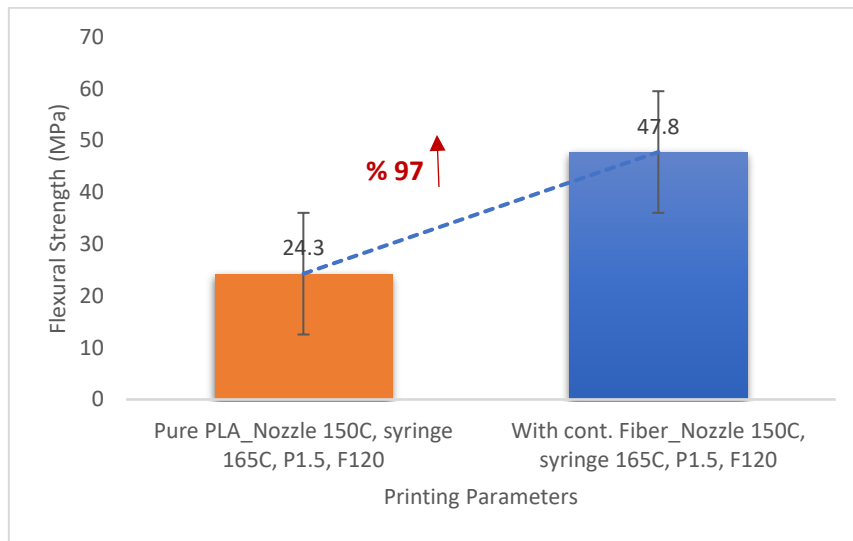


Figure 47: Flexure strength comparison of pure (left) and continuous carbon fiber reinforced PLA (right), with the parameters of; Nozzle temperature of 150°C, syringe temperature of 165°C, P 1.5 bar and F 120 mm/min.

According to the results, an approximately %97 improvement is observed with the continuous carbon fiber reinforced PLA, compared with the pure PLA samples.

3.2.3 Tensile following microwave oven application

The microwave oven was used as a post-processing technique to improve the thermal bonding between the printed layers. The samples with pure PLA and continuous carbon fiber reinforced PLA were performed separately.

For the pure PLA case; one of the separated samples, which has the length of 90 mm, was placed into the microwave oven at 800W power for 60 seconds. The obtained pairwise comparison result figures are presented in Figure 48, 49, and 50 respectively.

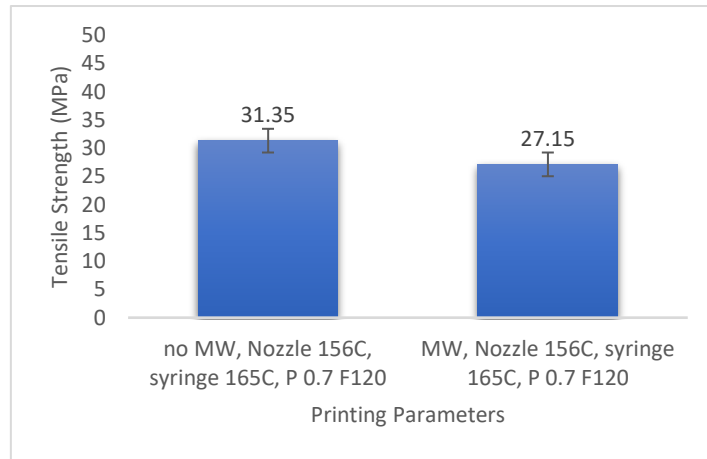


Figure 48: Tensile strength comparison of without microwave (left) and microwave treatment (right) for the parameters of Nozzle temperature of 156°C, syringe temperature of 165°C, P 0.7 bar and, F 120 mm/min.

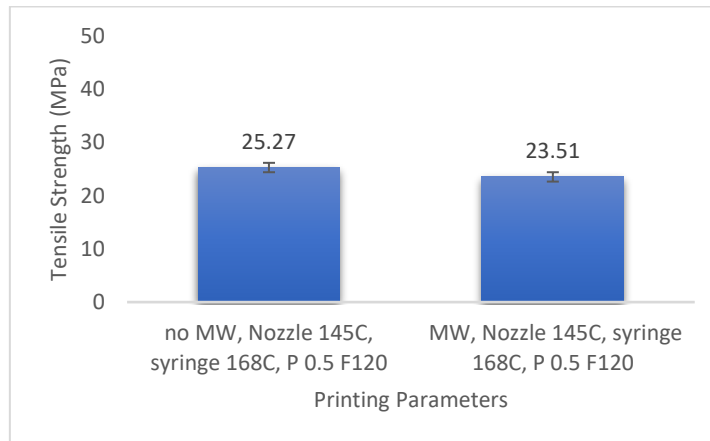


Figure 49: Tensile strength comparison of without microwave (left) and microwave treatment (right) for the parameters of Nozzle temperature of 145°C, syringe temperature of 168°C, P 0.5 bar and, F 120 mm/min.

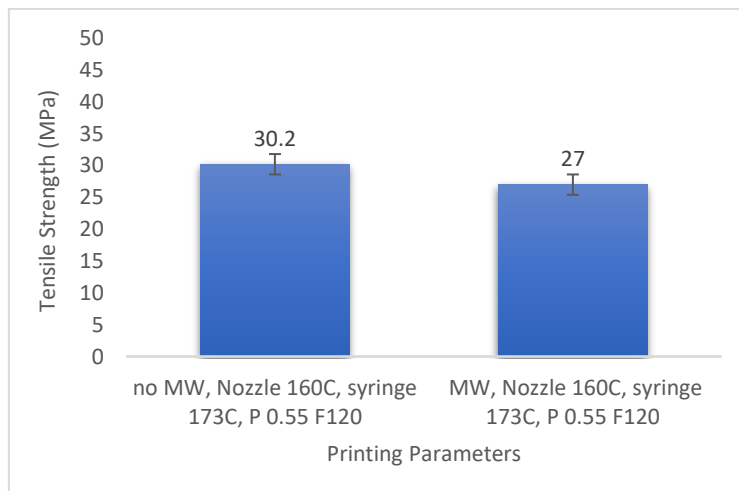


Figure 50: Tensile strength comparison of without microwave (left) and microwave treatment (right) for the parameters of Nozzle temperature of 160°C, syringe temperature of 173°C, P 0.55 bar and, F 120 mm/min.

As can be seen from the obtained results, for the pure PLA tensile strength tests, not much improvements were observed with the usage of the microwave oven. But, the breakage type of the tested samples changed. With using the microwave oven, instead of complete linear breakages, layer based breakages were observed.

For the continuous carbon fiber reinforced PLA samples; one of the separated sample, which has the same length as pure PLA (90 mm), was placed into the microwave oven at 300 Watt for 15 seconds. The obtained untreated and microwave utilized pairwise comparison results are presented in Figure 51.

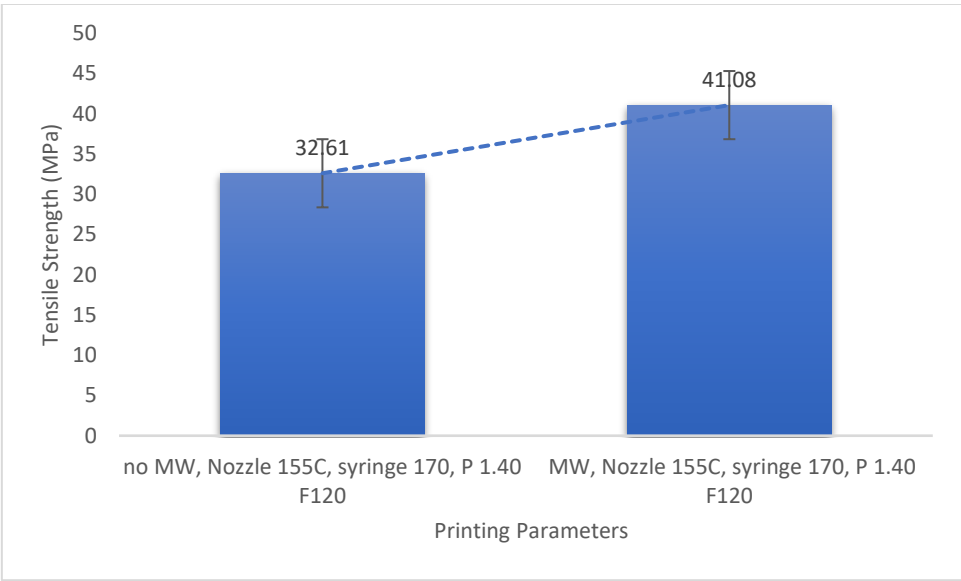


Figure 51: Tensile strength comparison of the untreated and the microwave treated continuous carbon fiber reinforced PLA samples.

Improvements were observed between the untreated and microwave used continuous carbon fiber reinforced PLA testes samples. The %26 increase was obtained based on the printing with parameters of Nozzle temperature of 155°C, syringe temperature of 170°C, P 1.4 bar and F 120 mm/min. Thus, it can be stated that the microwave oven can be used as a post-processing technique to enhance the tensile strength of the samples. By using the microwave oven, the thermal bonding of the materials can be improved and can result in stronger adhesion with higher tensile strength values. But, it is important to determine the appropriate microwave power and operation durations not to cause any damages to the samples.

3.2.4 Oxygen plasma application

After 3D printing of the oxygen plasma technique applied to the samples, the tensile test was performed to observe the effect of the method. As advised in the research papers by Tiwari et al. [55] and Kolluri et al. [57], the operation duration times of the oxygen plasma technique, were adjusted as 2 and 3 minutes, at 100W.

The tensile strength (MPa) results of the oxygen plasma treated cases for the printing parameters of; Nozzle temperature of 163°C, syringe temperature of 170°C, P 1.8 bar and, F 120 mm/min, were compared with the untreated continuous carbon fiber reinforced PLA (leftmost), as shown in Figure 52. The comparisons were performed with these printing parameter values because, these were the best printing parameters obtained by the comparison of tensile strength values of other printing parameters, which was shown in Figure 41.

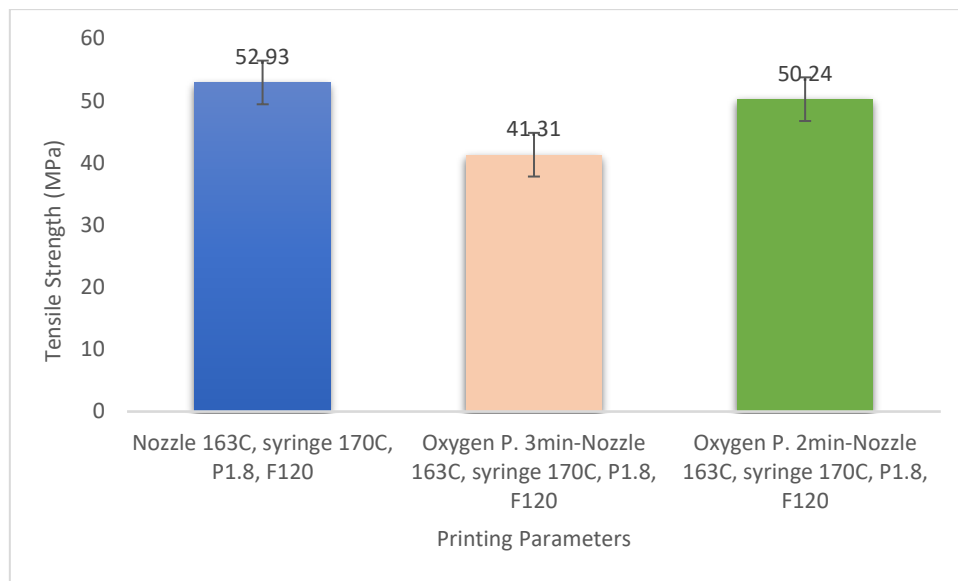


Figure 52: Tensile strength comparison of untreated (left), oxygen plasma 3 minutes treated (middle), and oxygen plasma 2 minutes treated (right) cases, for the same printing parameters of; Nozzle temperature of 163°C, syringe temperature of 170°C, P 1.8 bar and, F 120 mm/min.

Based on the obtained results from the tensile tests, it can be stated that the samples with oxygen plasma treated for 2 minutes result in higher tensile strength values than oxygen plasma treated for 3 minutes. In the comparison of 2 and 3 minutes treatment durations; by 2 minutes treatment, approximately %22 increase can be obtained, for the tensile strength values. This result shows

that 2 minutes oxygen plasma treatment to the continuous carbon fiber, performs better (%22 higher) when compared with 3 minutes treatments.

With the comparison of the untreated samples, the expected improvements cannot be observed with the oxygen plasma technique. The oxygen plasma application as pre-processing technique was a preliminary work and different power and duration parameters need be tested to observed more accurate results. Some of the reasons that prevented to obtain better results are; firstly, longer continuous carbon fiber piece was put inside of the oxygen plasma machine (Torr International Inc.), compared with the fibers used in the research paper of Tiwari et al. [55]. Although the fibers were put inside of the machine as much as in dissipated and spread position, because of the limited plate size of the machine, some fibers overlapped with each other. This can directly lower the process effectiveness. To increase the effectiveness of the process and obtain desired improvement values, depending on the used fiber amount, the power and operation duration time values, which was taken as 100W and 2-3 minutes, could be increased. Also, the printing process could not be performed immediately after the oxygen plasma treatment, the treated fibers were placed in the desiccator under the vacuum for 1 day, to preserve them from the direct contact with the air. This could also influence the results to obtain desired improvement values. Experiments need to be made with immediate printing to observe the effect. Oxygen plasma technique was a preliminary work and improvements can be done on this topic.

3.3 Fracture analysis of the tested samples

Observed breakages in tested samples of continuous carbon fiber reinforced and pure PLA, by using Tensile (ASTM D638) and Flexural (3-point bending, ASTM D790) tests, were also investigated. Based on the conducted mechanical tests, the fractured locations, analysis of the fractures such as; whether it is a valid fracture or not, were analyzed. Possible failure scenarios for the tensile test with stating failure's type, area, and location, is presented in Figure 53.

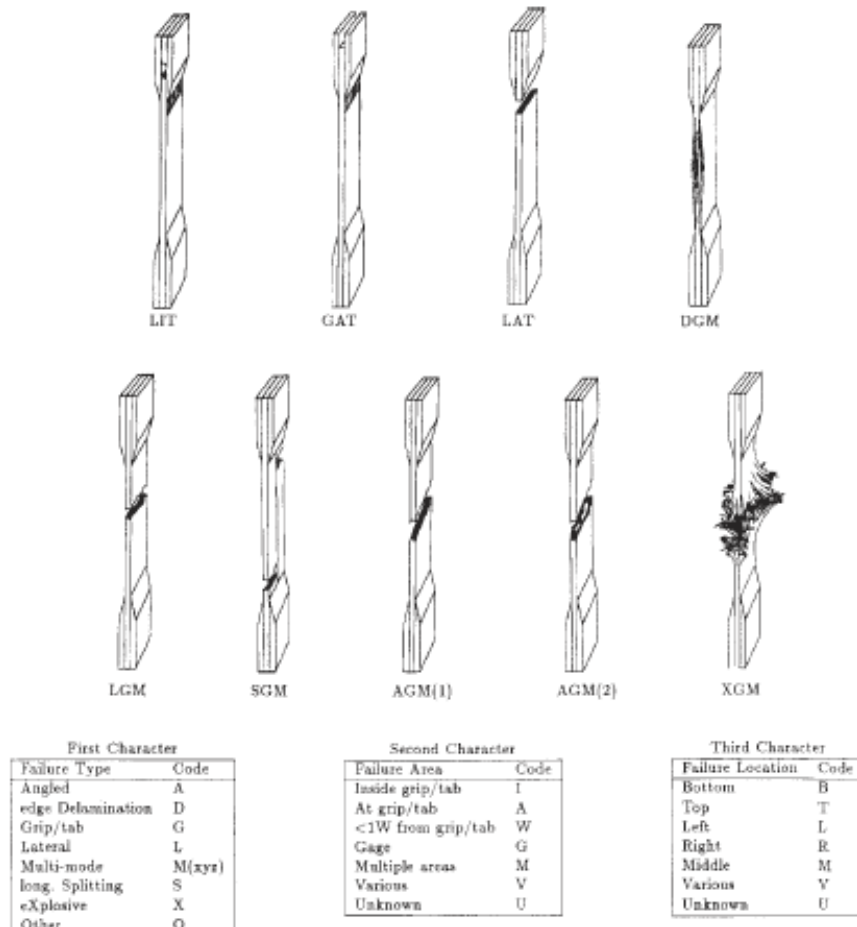


Figure 53: Possible tensile tested samples' failure scenarios and their codes [56].

According to the tensile test samples of pure PLA; the majority of the fractures were observed in the LAT and LGM forms (Figure 53), which symbolizes; lateral breakages close to tab that occurred in the top part of the samples, and lateral breakages in the gauge that occurred in the middle of the samples. Also, in some printed samples, the fractures occur in multiple areas and locations, and PLA was crumbled into pieces, at the end of the mechanical test. Because PLA has brittle structure, breakages happen very sharply during the mechanical test. Moreover, most of the tested pure PLA samples were separated into two or three sub-pieces, at the end of the performed tests. Thus, it can be stated that complete breakages of the thermoplastic material were observed, as a reason of its brittle characteristics. Also, for the most of the tested pure PLA samples, local breakages with linear alignments were observed.

Importantly, the amount of the used Araldite 2011-A/B adhesive, for the tab preparation and its pasting stage, had a great effect on the samples' breakages. Implemented Araldite's quantity

need to be equal as possible for all the tabs, to eliminate the occurrence of possible breakages due to the adhesive effect. The pasting stage needs to be carefully performed, and the fixed tabs need to be smooth. Otherwise, testing machine’s grips cannot hold and tighten the testing sample equally.

According to the tensile test samples of the continuous carbon fiber reinforced PLA; most of the breakages were observed in the explosive type of the scenarios; such as XGM coded form (Figure 53), which is explosive failures in the gauge, occurred in the middle part of the sample. The carbon fiber filaments were ruptured and failures occur in different sections of the samples. Some of the samples were ruptured on the bias (on the cross) and as a form of the staircase. It is observed that, when the small fracture occurs in the sample, it propagates easily and quickly, and breakages happen. Different from the tensile tested samples of pure PLA, for the carbon fiber reinforced samples separation into two sub-pieces was not generally observed. The continuous fibers inside of the samples were damaged and thermoplastic polymer as a matrix material was deformed and cracked, at the end of the mechanical tests. Some of the tensile tested carbon fiber reinforced PLA samples are presented in Figure 54.

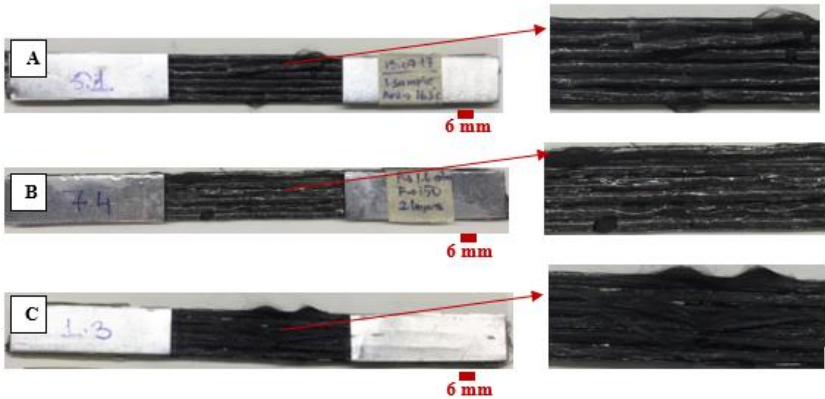


Figure 54: Tensile tested carbon fiber reinforced PLA samples’ fractures. (A) PLA cracks on surface and fibers are damaged, (B) PLA fractures and fiber pull-outs on the sides, and (C) fiber explosion.

As mentioned in the tensile test section, without tabs, the sample fracture cannot be observed in the defined gauge length and breakage occurs in the form of fiber pull-out, which is shown in Figure 55.



Figure 55: Without tabbed trial sample's observed fracture.

According to the flexural (3-point bending) tested samples of pure PLA; direct linear breakages are observed. Breakages occur where the force (F) is applied from the testing machine and instead of persisting on bending, breakages are formed and samples were separated. On the other hand; for flexural (3-point bending) tested samples of continuous carbon fiber reinforced PLA, the matrix material was deformed but, in most cases, the carbon fibers were not separated. At the end, the tested samples were curved with the applied force. Some of the flexural test samples for pure and continuous carbon fiber reinforced PLA can be seen in Figure 56.

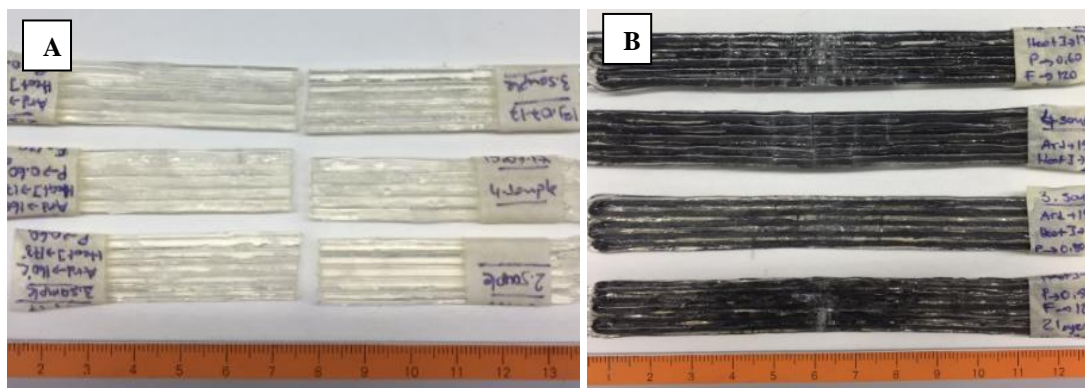


Figure 56: Flexural tested fractures. (A) pure PLA, and (B) continuous carbon fiber reinforced PLA samples.

Additionally, microwave oven used and unused pure and continuous carbon fiber reinforced PLA samples' fracture analysis were performed, individually. As the comparison between the tensile tested, microwave oven used and unused samples of pure PLA; with the implementation of the microwave, the failure type of the fracture was changed. By using a microwave, instead of complete linear breakages, layer based breakages and separations were observed. So, the samples were not fragmented and separated into sub-pieces, with the utilization of the microwave. The breakages of the microwave used pure PLA samples, is shown in Figure 57.

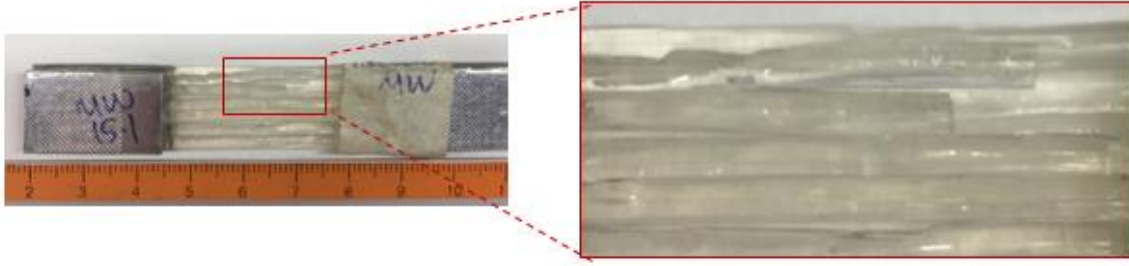


Figure 57: Tensile tested samples' fracture with the microwave oven usage as a post-processing technique.

Also, with the usage of the microwave oven in continuous carbon fiber reinforced PLA samples, breakage types were not changed. Similar to untreated samples, the carbon fiber filaments were ruptured and failures occurred in different sections of the samples.

Moreover, the performed tensile and flexural tests' continuous fiber breakages were examined under the Nikon Eclipse LV100ND optic microscope. Some of the observed fractures are presented in Figure 58.

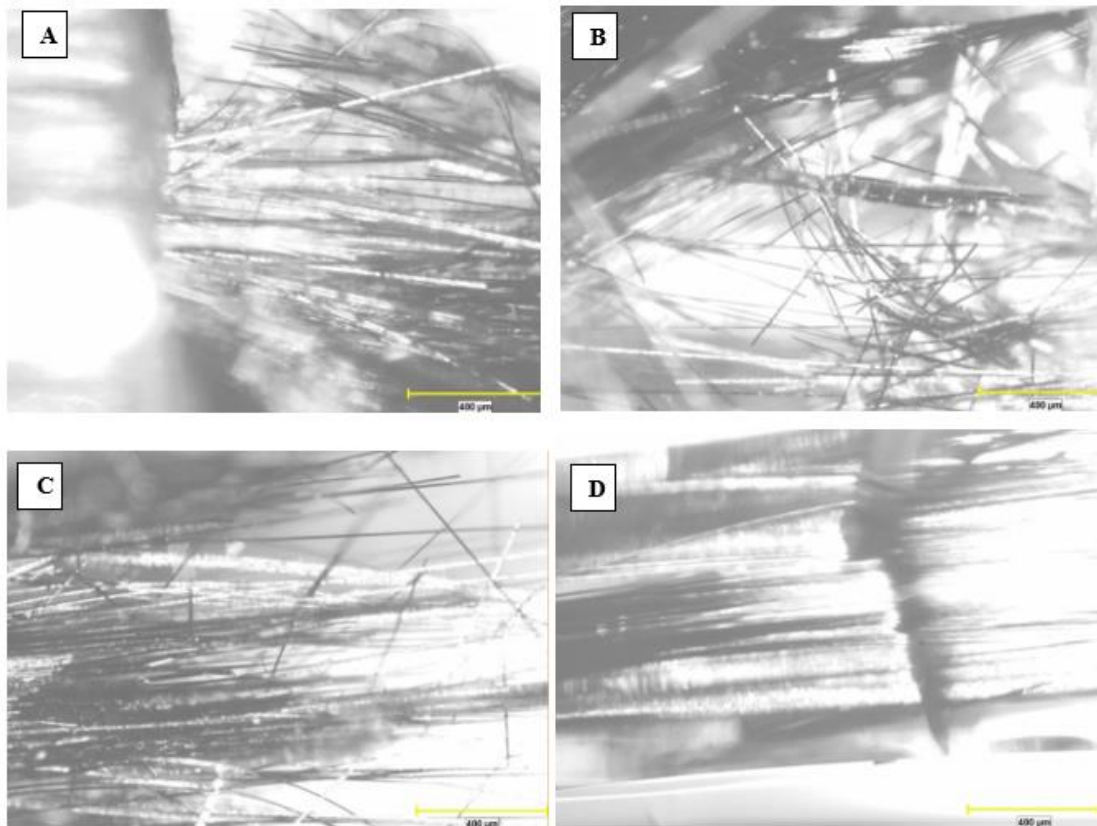


Figure 58: (A) fiber breakages observed in the tensile test with the magnitude 5X, (B) and (C) fiber breakages observed in the flexural test with magnitude 5X, in different perspectives and (D) fiber pull-out case in flexural test with magnitude 10X.

4. CONCLUSIONS & FUTURE WORKS

The main goal of this thesis is, to develop a FDM based coaxial additive manufacturing of continuous carbon fiber reinforced thermoplastic composite matrix, for improving the mechanical properties of the 3D printed parts, which can extend the restricted application area to a functional end-parts. The effect of using continuous carbon fibers as a reinforcement and PLA 4043D as thermoplastic matrix material was analyzed by 3D printing of both, carbon fiber reinforced and pure PLA samples to examine the improvements. The initial step of the project was to develop and modify the coaxial nozzle and implementing for the developed printing setup. After the 3D printing process of the samples, the tensile and flexural (3-point bending) mechanical tests were performed according to the ASTM D638 and ASTM D790 standards, respectively. The mechanical tests were conducted separately for both, the continuous carbon fiber reinforced and pure PLA samples, to able to compare their resulted values.

Optical microscope and scanning electron microscope (SEM) methods are used for the visualization of fracture surfaces. Based on the experiments, when the printed samples mean values were taken and according to the tensile strength test, approximately %42 improvement was obtained with the usage of carbon fiber as a reinforcement. But, this improvement results can increase %112 with the experiments conducted by using the same printing parameters, to show the exact effect of using continuous carbon fibers. Also, diffusion and adhesion problems were observed between the printed layers and stripes, which are the main problems observed with carbon fiber usage in 3D printing. To achieve perfect reinforcement from the continuous carbon fiber, fiber need to be fully embedded in PLA matrix, which could significantly improve the mechanical strength of the part. Additionally, more voids were observed with the continuous carbon fiber reinforced PLA than the pure PLA samples, which could have a direct effect on the mechanical performance of the printed part.

Due to the diffusion and adhesion problems between the continuous carbon fiber and PLA as a thermoplastic material, a weak integration and bonding between the materials were observed. The reason behind the diffusion problem is related to the supplied continuous carbon fibers' jointly (without distributed) deposition from the nozzle. So, the molten PLA thermoplastic materials, cannot fully diffuse inside of the fiber and cannot achieve an ideal composite

reinforced-matrix form. Hence, the future work of this thesis needs to focus on the continuous carbon fibers' spreading methods before the 3D printing. With spreading, PLA can be perfectly integrated with the fiber, which could increase the mechanical properties. The nozzle can be redesigned to spread the supplied continuous carbon fiber, before the 3D printing process. By adding a new spreading part to the current design, fibers can be separated and diffusion of PLA material can be achieved during the printing. An exemplary view of the fiber spreading can be seen in Figure 59.

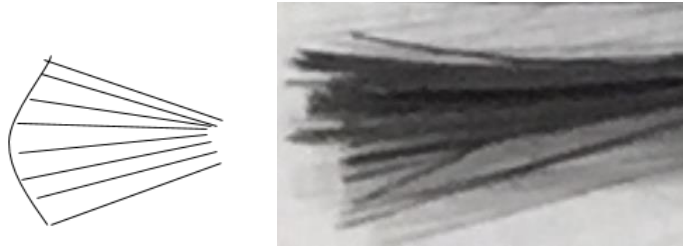


Figure 59: Presentation of spread-out continuous carbon fiber.

Additionally, as a future work, other pre-processing techniques can be applied to the fiber and more investigations can be made on the fiber surface treatments. By applying effective surface treatment to the continuous carbon fiber, the adhesion properties between fiber and PLA can be improved. Even the small improvement on this issue can pave the way for greater mechanical results. Furthermore, 3D printing operation can be repeated with a smaller nozzle diameter to understand the effect of the nozzle diameter on the adhesion between the materials.

In this thesis, PLA thermoplastic matrix material was investigated because it is commonly used in 3D printing and also it is bio-degradable. However, other thermoplastic polymers (such as ABS, PEEK and Nylon) can be used by modifying the current developed nozzle and the system. Also, instead of supplying PLA pellets from a single polymer syringe which is located on the side, the design can be modified to feed the thermoplastic material equally from all the directions, which could result in higher bonding properties between the materials and better mechanical test values. Moreover, screw based design can be developed and implemented into the system. By having a screw based system for feeding the thermoplastic pellets into the liquefier, the 3D printing process of larger parts can be made. As another important point, during the printing operation, stretching of the carbon fibers can be investigated with experiments and its effect on the mechanical improvement could be observed.

References

1. Duty, C., et al., *Structure and mechanical behavior of Big Area Additive Manufacturing (BAAM) materials*. Rapid Prototyping Journal, 2017. **23**(1): p.181-189.
2. Post, B., et al., *The Economics of Big Area Additive Manufacturing*. Solid Freeform Fabrication 2016: Proceedings of the 27th Annual International Solid Freeform Fabrication Symposium- An Additive Manufacturing Conference, 2016. p. 1176-1182.
3. Xiaoyong, S., et al., *Experimental Analysis of High Temperature PEEK Materials on 3D Printing Test*. 9th International Conference on Measuring Technology and Mechatronics Automation, 2017. p. 13-16.
4. Prüß, H., et al., *Design for Fiber-Reinforced Additive Manufacturing*. Journal of Mechanical Design, 2015. **137**: p. 1-7.
5. Tian, X., et al., *Interface and performance of 3D printed continuous carbon fiber reinforced PLA composites*. Composites: Part A, 2016. **88**: p. 198–205.
6. Chapiro, M., *Current achievements and future outlook for composites in 3D printing*. Reinforced Plastics, 2016. **00**(00): p. 1-4.
7. Zemcik, O., et al., *A Distribution of Temperature Field in the FDM Printhead*. New Technologies in Manufacturing, 2011. p. 1-5.
8. Sukindar, N., et al., *Analysis on Temperature Settings for Extruding Polylactic Acid Using Open-Source 3D Printer*. ARPN Journal of Engineering and Applied Sciences, 2017. **12**(4): p. 1348-1353.
9. Love, L., et al., *The importance of carbon fiber to polymer additive manufacturing*. Journal of Materials Research, 2014. **29**(17): p. 1893-1898.
10. Ning, F., et al., *Additive manufacturing of carbon fiber reinforced thermoplastic composites using fused deposition modeling*. Composites Part B, 2015. **80**: p. 369-378.
11. Li, N., et al., *Rapid prototyping of continuous carbon fiber reinforced polylactic acid composites by 3D printing*. Journal of Materials Processing Technology, 2016. **238**: p. 218–225.
12. Melenka, G., et al., *Evaluation and prediction of the tensile properties of continuous fiber-reinforced 3D printed structures*. Composite Structures, 2016. **153**: p. 866-875.

13. Sukindar, N., et al., *Analyzing the effect of nozzle diameter in Fused Deposition Modelling for extruding Polylactic Acid using open source 3D Printing*. Jurnal Teknologi, 2016. **78**(10): p. 7-15.
14. Jerez- Mesa, R., et al., *Finite element analysis of the thermal behavior of a RepRap 3D printer liquefier*. Mechatronics, 2016.**000**: p. 1-8.
15. Ramanath, H., et al., *Melt flow behaviour of poly-e-caprolactone in fused deposition modelling*. Journal of Materials Science: Materials in Medicine, 2008. **19**: p. 2541-2550.
16. Sa'ude, N., et al., *Melt Flow Behavior of Metal Filled in Polymer Matrix for Fused Deposition Modeling (FDM) Filament*. Trans Tech Publications: Applied Mechanics and Materials, 2014. **660**: p. 84-88.
17. Carneiro, O., et al., *Fused deposition modeling with polypropylene*. Materials & Design, 2015. **83**: p. 768- 776.
18. Halli, M., et al., *Design and Implementation of Arduino based 3D Printing using FDM Technique*. International Journal of Research in Engineering and Technology, 2016. **05**(04): p. 182-185.
19. Ibrahim, M., et al., *Verification of Feed Rate Effects on Filament Extrusion for Freeform Fabrication*. ARPN (Asian Research Publishing Network) Journal of Engineering and Applied Sciences, 2016. **11**(10): p. 6556-6561.
20. Girdis, J., et al., *Additive Manufacturing of Carbon Fiber and Graphene- Polymer Composites using the technique of Fused Deposition Modelling*. Solid Freeform Fabrication: Proceedings of the 27th Annual International Solid Freeform Fabrication Symposium-An Additive Manufacturing Conference Reviewed Paper, 2016. p. 864-870.
21. Fernandez, S., et al., *Additive Manufacturing and Performance of Functional Hydraulic Pump Impellers in Fused Deposition Modeling Technology*. Journal of Mechanical Design, 2016. **138**(024501): p. 1-4.
22. Chuang, K., et al., *Additive Manufacturing and Characterization of Ultem Polymers and Composites*. CAMX Conference Proceedings- The Composites and Advanced Materials Expo., 2015.
23. Hwang, S., et al., *Thermo-mechanical Characterization of Metal/Polymer Composite Filaments and Printing Parameter Study for Fused Deposition Modeling in the 3D Printing Process*. Journal of Electronic Materials, 2015. **44**(3): p. 771-777.
24. Ning, F., et al., *Additive Manufacturing of CFRP Composites Using Fused Deposition Modeling: Effects of Carbon Fiber Content and Length*. Proceedings of the ASME

- International Manufacturing Science and Engineering Conference, MSEC, 2015. p. 1-7.
25. Wittbrodt, B., et al., *The Effects of PLA Color on Material Properties of 3-D Printed Components*. Additive Manufacturing, 2015. **8**: p. 1- 17.
26. Brenken, B., et al., *Fused Deposition Modeling of Fiber- Reinforced Thermoplastic Polymers: Past Progress and Future Needs*. 2016. Retrieved from <https://mech.utah.edu/ASC2016/assets/0203.pdf>
27. Lindberg, J., et al., *Simulating Thermoplastic Flow Through a 3D Printer Nozzle*. Journal of Undergraduate Chemical Engineering Research, 2016. **5**: p. 61-66.
28. Holshouser, C., et al., *Out of Bounds Additive Manufacturing*. Advanced Materials and Processes, 2013. p. 15-17.
29. Beyer, C., *Strategic Implications of Current Trends in Additive Manufacturing*. Journal of Manufacturing Science and Engineering, 2014. **136**: p. 1-8.
30. Taylor, A., et al., *System and Process Development for Coaxial Extrusion in Fused Deposition Modelling*. Rapid Prototyping Journal, 2017. **23**(3): p. 1-12.
31. Turner, B., et al., *A review of melt extrusion additive manufacturing processes: I. Process design and modeling*. Rapid Prototyping Journal, 2014. **20**(3): p. 192-204.
32. Agarwala, M., et al., *Structural quality of parts processed by fused deposition*. Rapid Prototyping Journal, 1996. **2**(4): p. 4-19.
33. Earls, A., et al., *The road ahead for 3-D printers*. PwC Technology Forecast, 2014. **2**: p. 1-10.
34. Wu, W., et al., *Influence of Layer Thickness and Raster Angle on the Mechanical Properties of 3D-Printed PEEK and a Comparative Mechanical Study between PEEK and ABS*. Materials, 2015. **8**: p. 5834-5846.
35. Bual, G., et al., *Methods to Improve Surface Finish of Parts Produced by Fused Deposition Modeling*. Manufacturing Science and Technology, 2014. **2**(3): p. 51-55.
36. van der Klift, F., et al., *3D Printing of Continuous Carbon Fibre Reinforced Thermoplastic(CFRTP) Tensile Test Specimens*. Open Journal of Composite Materials, 2016. **6**: p. 18-27.
37. Matsuzaki, R., et al., *Three-dimensional printing of continuous- fiber composites by in-nozzle impregnation*. Scientific Reports, 2016. **6**: p. 1-7.

38. Bade, L., et al., *Investigations into the Development of an Additive Manufacturing Technique for the Production of Fibre Composite Products*. Procedia Engineering, 2015. **132**: p. 86-93.
39. Namiki, M., et al., *3D Printing of Continuous Fiber Reinforced Plastic*. 2014. Retrieved from https://www.researchgate.net/publication/286005621_3D_printing_of_continuous_fiber_reinforced_plastic
40. Naidu, D., et al., *Experimental Determination of Mechanical Properties of ABS Material Components Made by RP Manufacturing Technique*. International Journal of Recent Advances in Multidisciplinary Research (IJRAMR), 2015. **2**(12): p. 1012-1015.
41. Rahman, K., et al., *Mechanical Properties of Additively Manufactured PEEK Components Using Fused Filament Fabrication*. Proceedings of the ASME International Mechanical Engineering Congress and Exposition (IMECE), 2015. p. 1-11.
42. Berman, B. *3-D printing: The new industrial revolution*. Business Horizons, 2012. **55**: p. 155- 162.
43. Tekinalp, H., et al., *Highly oriented carbon fiber-polymer composites via additive manufacturing*. Composites Science and Technology, 2014. **105**: p. 144-150.
44. Quan, Z., et al., *Additive manufacturing of multi-directional preforms for composites: opportunities and challenges*. Materials Today, 2015. **00**(00): p. 1-10.
45. Belter, J., et al., *Strengthening of 3D Printed Fused Deposition Manufactured Parts Using the Fill Compositing Technique*. PLOS ONE, 2015. **10**(4): p. 1-19.
46. Wang, X., et al., *3D printing of polymer matrix composites: A review and prospective*. Composites Part B, 2017. **1**(10): p. 442-458.
47. Bettini, P., et al., *Fused Deposition Technique for Continuous Fiber Reinforced Thermoplastic*. Journal of Materials Engineering and Performance, 2016. p. 1-6.
48. Mohan, N., et al., *A review on composite materials and process parameters optimisation for the fused deposition modelling process*. Virtual and Physical Prototyping, 2017. **12**(1): p. 47-59.
49. Bala, A., et al., *Elements and Materials Improve the FDM Products: A Review*. Advanced Engineering Forum, Trans Tech Publications, 2016. **16**: p. 33-51.
50. *Chapter 6: Innovating Clean Energy Technologies in Advanced Manufacturing Technology Assessments*. U.S. Department of Energy, Quadrennial Technology Review, 2015. p. 1-35.

51. Nakagawa, Y., et al., *3D printing of carbon fibre-reinforced plastic parts*. International Journal of Advanced Manufacturing Technology, 2017. **91**: p. 2811-2817.
52. *3K A-38 Technical Data Sheet*. 2016. Retrieved from <http://www.dowaksa.com/wp-content/uploads/2017/04/3K-A-38.pdf>
53. *ASTM D638 Type I*. 2014. Retrieved from https://www.datapointlabs.com/Images/Specimens/ASTM_D638_TypeI.pdf
54. Advanced Materials, *Huntsman Araldite 2011-A/B Multi-Purpose Epoxy Adhesive*. 2007. p. 1-6. Retrieved from <http://www.dawex.cz/userFiles/technicke-listy/huntsman/araldite-2011.pdf>
55. Tiwari, S., et al., *Surface Treatment of Carbon Fibers - A Review*. Procedia Technology, 2014. **14**: p. 505-512.
56. ASTM D3039/D 3039M-00. *Standard Test Method for Tensile Properties of Polymer Matrix Composite Materials*. ASTM International, West Conshohocken, 2000. p. 1-13.
57. Kolluri, O., et al., *Gas Plasma and the treatment of Advanced Fibers*. Society of Plastics Engineers Advanced Polymer Composites, 1988. p. 1-8.
58. *Ingeo Biopolymer 4043D Technical Data Sheet Biaxially Oriented Films-General Purpose*. NatureWorks. p. 1-4.